

McAlpine, J.D. and M. Ruby. 2008. *Computational Fluid Dynamics of Microscale Meteorological Flows for Air Quality Applications*. Chapter 5C of *AIR QUALITY MODELING - Theories, Methodologies, Computational Techniques, and Available Databases and Software. Vol. III – Special Issues* (P. Zannetti, Editor). Published by The EnviroComp Institute (<http://www.envirocomp.org/>) and the Air & Waste Management Association (<http://www.awma.org/>).

Chapter 5C

Computational Fluid Dynamics of Microscale Meteorological Flows for Air Quality Applications

J.D. McAlpine ⁽¹⁾ and Michael Ruby ⁽²⁾

⁽¹⁾ *Envirometrics, Inc., Seattle, Washington (USA)*

jdmcalpine@envirometrics.com

⁽²⁾ *Envirometrics, Inc., Seattle, Washington (USA)*

mruby@envirometrics.com

Abstract: There is an ever-increasing need to simulate airflow at the micro-meteorological scale for environmental applications. Dispersion of pollutants around buildings and pedestrian level wind-speeds are two applications that concern environmental planners. Wind tunnels are still the main tool used, but computational methods are becoming more popular as a way to address these issues. Computational Fluid Dynamics (CFD) simulations are being used more often to model the surface layer of the atmosphere for environmental application. The use of CFD in this field is still experimental in nature and inherent weaknesses are apparent, but advances in computing and simulation methods are continually driving it towards becoming a reliable tool for predicting local air quality and other environmental conditions.

This review addresses today's common method of simulating the atmospheric surface layer in an urban environment using CFD. The features of the surface layer that are important for flow modeling are discussed as well as different methods for applying them in CFD. Different turbulence models and techniques for simulating the surface layer in CFD are reviewed as well. Current guidelines and processes for conducting a project are also described and discussed.

This chapter is intended for environmental scientists or engineers as an overview of the basics of CFD and its application to the surface layer of the atmosphere so that one can know how to conduct or evaluate a CFD analysis for compliance with industry best practices.

Key Words: CFD, micrometeorology, air quality, atmosphere, surface layer, buildings, urban, turbulence, modeling, Computational Fluid Dynamics, K-epsilon, steady state flow, plume, pollution, guidelines, ERCOFTAC, QNET-CFD, dispersion, validation, Computational Wind Engineering, RNG, lab hood, stacks, airflow, Chen-Kim, Project EMU.

1 Introduction

Air quality modeling has become an important tool for environmental review. Gaussian dispersion models and puff models are now routinely used to model the dispersion of pollutants from industry and traffic as part of regulatory and voluntary efforts to ensure that we breathe healthy air. Air quality models are invaluable in their ability to help planners assess the likely environmental impacts from alternative configurations of sources.

Lately, there has been increasing interest in addressing air quality at the local scale, in and around homes and workplaces. Recent issues such as sick building syndrome, the carcinogenicity of diesel particulate matter, terrorist attacks using chemical or biological weapons, and accidental chemical spills have especially driven this interest. Air quality modeling of the dispersion of pollutants through the urban landscape is needed to study these issues.

Traditional air quality models such as the Industrial Source Complex-Short Term (ISCST3) model can not adequately handle dispersion around a building. The “PRIME” addition to these models has been applied to account for the influence of building wakes on pollutant concentrations downwind of buildings, but not concentrations on the building itself, such as at air intakes.

Atmospheric boundary layer wind tunnels have been the dominant tool for modeling the dispersion of exhaust at the local scale. The U.S. Environmental Protection Agency (EPA) has a set of standards for fluid modeling of the atmosphere that lends guidance for these efforts (Snyder, 1981), and it is today’s accepted method for local scale air quality and environmental analysis. Though proven and reliable, wind tunnel modeling can be expensive and time consuming, and thus unjustifiable for simpler studies. The number of installations available for wind tunnel modeling is also quite limited, with just a handful of commercial facilities available.

Computational Fluid Dynamics (CFD) shows promise as a tool for answering questions about local air quality in and around buildings by providing computerized simulation models. CFD works by solving the fundamental equations of motion using assumptions about local turbulence to obtain a steady-state or time-dependent airflow structure in a domain. Therefore, it is essentially a computerized, virtual wind tunnel.

For example, in a typical local-scale air quality project using CFD, one would first essentially “build” the domain of the project by assigning boundaries representing buildings, vegetation, pollutant sources, and other features. Second, additional boundary conditions would be assigned to represent air inlets and outlets to the domain, with careful attention to match incoming wind and turbulence profiles to a typical atmospheric condition. The domain is then “meshed”; that is, divided into a three dimensional grid of discrete volumes, as illustrated in Figure 1, that the CFD solver will use to compute changes in fluid motion through discrete finite difference calculations. After this, a field initialization would be prescribed. The CFD model solver is then run until a steady state solution is reached or for a set amount of time to an unsteady-state solution. The results would then be viewed in a graphical user interface for analysis. Wind vectors, plume paths, turbulent kinetic energy, and pollutant concentrations would be typical variables for exploration.

Modeling of flow around buildings is typically referred to as Computational Wind Engineering and covers several applications including pollutant dispersion, pedestrian wind evaluation, building wind loading, and snow loading. This chapter focuses primarily on the details of simulating the steady-state atmospheric surface layer in the CFD domain for the dispersion of pollutants in and around buildings.

This chapter is divided into four sections:

- Synopsis of CFD: the math, assumptions, and availability.
- Simulation of the atmosphere in CFD
- Application of the method and guidelines
- Verification and validation efforts

This chapter does not explore the mathematics behind CFD in depth, but rather, it is meant to help the environmental scientist or engineer understand the basics of CFD and its applications to the atmospheric boundary layer. It should provide sufficient information on the strengths and weaknesses of the method to allow a thorough review of a CFD project.

A more basic introduction to CFD modeling for air quality applications, with illustrations of example projects using CFD, has been provided previously by the authors (McAlpine and Ruby, 2004).

2 Synopsis of CFD: the Math, Assumptions, and Availability

To begin discussing the basics of CFD, we must first explore the nature of fluid flow, and thus, the basic equations of fluid motion as applied to the atmosphere. CFD works by solving the equations of motion using several assumptions about the local behavior of turbulence. First, in this section we will derive the equations

of motion and the turbulence terms that will make the solution possible. Then, we will explore the turbulence assumptions that are needed when solving the equations. We will discuss how CFD is set up to solve these equations, and finally, we will describe guidelines for modeling and validating a CFD code using a standard problem.

2.1 Equations of Motion

The basic equations of motion are applicable to any type of fluid flow, but we will focus on an atmospheric application of the equations in illustrating how CFD works. First, we will explore the fundamentals of what is happening at a point in a hypothetical two-dimensional atmosphere. We will consider a discrete volume of the atmospheric surface layer, as illustrated in Figure 1. The change in velocity across our volume will be influenced by several factors: 1) the local horizontal pressure gradient and the velocity of air entering our domain will influence our local velocity; 2) air above our volume will be moving at a higher velocity than the air below our volume since our volume is located in a horizontal wind that changes in the vertical with profile $U(z)$; and 3) diffusion of momentum into and out of our volume.

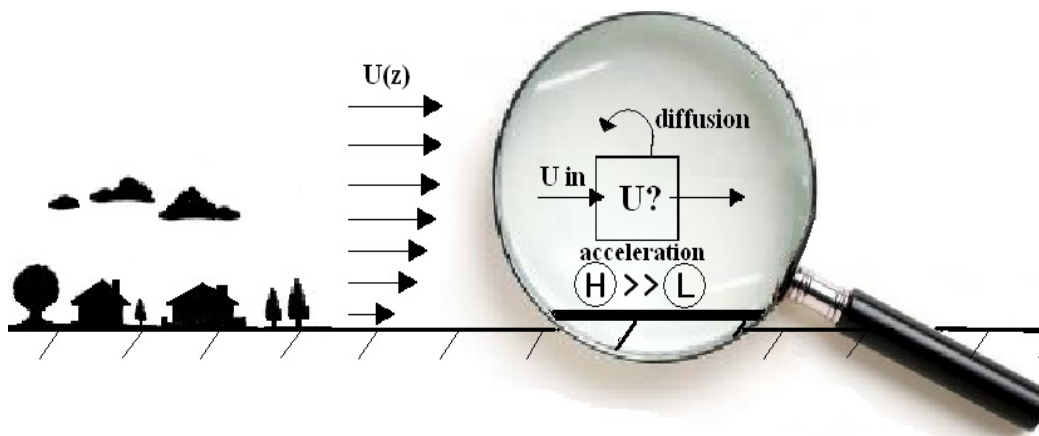


Figure 1. Examination of a volume of air in the atmospheric boundary layer of wind profile $U(z)$. The local change of velocity in our volume is dependent on the pressure gradient (represented in the graphic as Higher pressure going to Lower pressure) and transport of velocity through molecular and turbulent diffusion.

The higher velocity above and the slower velocity below, our volume will create stress that will force the kinetic energy in our volume to diffuse downward as turbulence. Similarly, turbulence will diffuse downward into our volume from above.

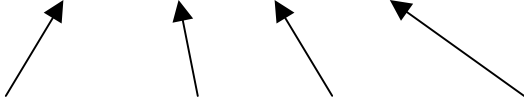
Since we are interested in modeling the velocity of wind flow in a discrete volume of the atmosphere, we need to establish equations of motion for the local change in velocity at this point. One of the more important features of our

atmospheric volume will be the difference in pressure in the horizontal due to local atmospheric weather systems.

This pressure difference is a force that results in advection of air and its velocity into our volume and an acceleration of the air mass, resulting in a change in velocity. Writing out the conservation of momentum equation for our volume, we have:

$$\begin{aligned} \text{Local change of velocity} = & \text{advection of velocity} + \text{turbulent diffusion of velocity} \\ & + \text{acceleration from pressure gradient} \end{aligned}$$

For the 2-D case, the equation for the u-component of velocity per unit density will be:

$$\frac{\partial \mathbf{u}}{\partial t} = -\mathbf{u} \frac{\partial \mathbf{u}}{\partial x} + \nu \frac{\partial^2 \mathbf{u}}{\partial z^2} - \frac{1}{\rho} \frac{\partial P}{\partial x} \quad (2.1)$$


Local change of velocity = advection + turbulent diffusion + acceleration

where \mathbf{u} is the velocity vector, P is the pressure, and ν is the sum of molecular and turbulent viscosity of air.

Conservation of mass comes into play through the continuity equation. Let us assume that in our hypothetical atmosphere the density variations are small enough to ignore. This is a good assumption for the neutral and stable atmospheric surface layer, where the flow is virtually incompressible and isothermal on a small scale. It is also reasonable to assume that air is an incompressible fluid in the atmospheric boundary layer (Garratt, 1992). Thus, we can write an equation that says the instantaneous velocity divergence is zero across the flow:

$$\frac{\partial \mathbf{u}}{\partial x} = 0 \quad (2.2)$$

These two equations (2.1 and 2.2) together are known as the Navier-Stokes equations. Variations of these two equations can be used for any type of fluid flow. Gravity and the Coriolis force are not included in these equations because at the local scale (i.e., not much more than 1 km) in the neutral atmosphere these terms are negligible. More importantly, these two equations, in this form, do not suggest any turbulence, a primary feature of local atmospheric flows.

2.2 Reynold's Averaging

Turbulent flow in the atmospheric boundary layer is, by its nature, one of chaos. Therefore, modeling the exact, turbulent velocity in the atmosphere at any given moment would be extremely difficult. Modeling only the mean flow at any given moment is the usual approach in larger scale modeling of atmospheric flows. However, mean flow does not tell us anything about the turbulent fluctuations in the flow. Because turbulence is the dominant feature of the boundary layer on the local scale, we must address it. A statistical approach has been found to be a good way to approach turbulent modeling.

“Reynold's decomposition” is the separation of the instantaneous velocity into its mean and fluctuating parts (Arya, 1988):

$$\mathbf{u} = \bar{\mathbf{u}} + \mathbf{u}' \quad (2.3)$$

where u' is the deviation from the mean flow (\bar{u}) and represents the turbulent flux of velocity. Figure 2 demonstrates the measurement of u' and the mean velocity in the atmosphere. The standard deviation of the flow (σ_u) is a measure of this variance:

$$\sigma_u = \sqrt{u'^2} \quad (2.4)$$

The turbulent fluctuations are extremely important, especially in air pollution modeling, because turbulent flux is the dominant transport term of scalar flux.

Reynold's averaging can now be incorporated into the Navier-Stokes equations by substituting the mean component and fluctuating component into each variable and then averaging each term. We will not here go through the mathematics of Reynold's averaging. We will just state that terms, such as $\overline{\mathbf{u} \mathbf{w}'}$ and $\overline{\mathbf{u} \mathbf{u}'}$, drop out of the equation because the average of a fluctuating component is zero. A good mathematical demonstration of Reynold's averaging of the conservation of momentum equation can be found in several textbooks (e.g., Stull, 1988).

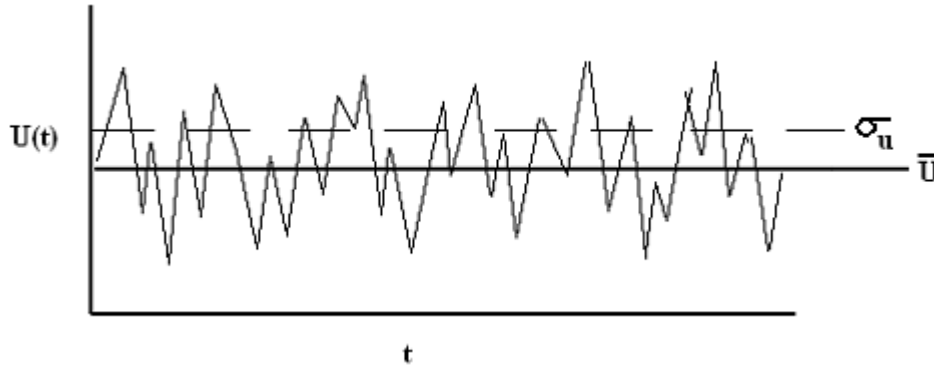
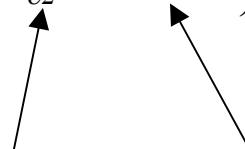


Figure 2. Graph of wind speed observation at a fixed point with time. Modeling of the flow can be simplified by Reynolds decomposition.

The result is the Reynold's averaged Navier-Stokes (RANS) equations, which contain two new unknowns representing turbulence, $\overline{u'u'}$ and $\overline{u'w'}$. These are known as the “Reynold's stresses”. The RANS equations now include the conservation of mass equation (2.2) and a rewritten conservation of momentum equation (2.5):

$$\frac{\partial \mathbf{u}}{\partial t} = -\overline{\mathbf{u}} \frac{\partial \overline{\mathbf{u}}}{\partial x} + \frac{\partial}{\partial z} \left(\nu \frac{\partial \overline{\mathbf{u}}}{\partial z} + \overline{\mathbf{u}'\mathbf{u}'} + \overline{\mathbf{u}'\mathbf{w}'} \right) - \frac{1}{\rho} \frac{\partial P}{\partial x} \quad (2.5)$$



 molecular diffusion turbulent diffusion

In this two-dimensional example, we now have two equations and 4 unknowns: $\overline{\mathbf{u}}$, $\overline{\mathbf{w}}$, $\overline{\mathbf{u}'\mathbf{u}'}$, and $\overline{\mathbf{u}'\mathbf{w}'}$. Vertical velocity, w , is still considered an unknown in the equation even though we are assuming it is zero, and thus not displaying the term $-\overline{\mathbf{w}} \frac{\partial \overline{\mathbf{u}}}{\partial z}$ in the equation.

To make these equations solvable, we need to find additional equations that will relate the turbulence terms to the properties of the mean flow. This is known as “turbulence closure.” Several different turbulence closure techniques have been proposed using various assumptions about turbulence, but none has ever proved entirely satisfactory (Arya, 1988).

2.3 Turbulence Closure

Assumptions must be made about turbulence to model the turbulent fluctuations and solve the equations of motion. Equations that relate the unknown turbulent

variances to the mean flow must be proposed. We can first explore this by stepping back to our earlier discussion, where we noted that turbulent fluctuations are carried down-gradient from higher velocity to lower velocity. From this observation we are led to the assumption that the turbulent stress is proportional to the velocity gradient in some way:

$$\overline{\mathbf{u}'\mathbf{w}'} = ? \cdot \frac{\partial \bar{\mathbf{u}}}{\partial z} \quad (2.6)$$

where ? indicates an unknown proportionality constant or variable.

At a very small scale in viscous liquid fluids, Isaac Newton proposed and confirmed that molecular turbulent shearing stress is linearly proportional to the velocity gradient:

$$\frac{\tau}{\rho} = \nu \frac{\partial \bar{\mathbf{u}}}{\partial z} \quad (2.7)$$

where τ is the shear stress of the fluid, and ν is a constant known as molecular kinematic viscosity, which is unique for each fluid. If we assume that turbulent viscosity in the atmosphere is analogous to molecular viscosity, as J. Boussinesq did in 1877, then we have a solution relating the turbulent stresses to the mean flow (Arya, 1988):

$$\frac{\tau}{\rho} = \overline{\mathbf{u}'\mathbf{w}'} = -K \frac{\partial \bar{\mathbf{u}}}{\partial z} \quad (2.8)$$

Making this assumption is known as “K theory.” The constant K can be considered the turbulent viscosity of the fluid, ν_t . However, it has been found that this assumption by analogy is flawed; turbulent stress is not linearly proportional to the gradient of the flow in some cases. In the surface layer of the atmosphere, the linear assumption is acceptable in neutral and slightly stable conditions over open areas, but it breaks down as soon as the flow interacts with buildings and obstacles, or the atmosphere becomes unstable, generally because it cannot account for the energy stored in large eddies. Also, in some cases, turbulent fluctuations can transfer up-gradient to higher velocity due to large eddies. Therefore, to be more accurate and to ensure equation closure, the turbulent viscosity assumption must be able to change with location and still be defined by properties of the flow.

A different assumption can be derived from dimensional analysis, a favorite tool of engineers (and first used in exploring turbulent flow). Using dimensional analysis, we note that the units of K must be (length²/time) or m²/s. Prandtl hypothesized in 1925 that this mixing length scale can be defined as the average

distance a parcel of air moves when it is displaced, and that it is a function of height and atmospheric state. It was then proposed that a good estimate for this length in a neutral atmosphere is $L = kz$, where k is the Von Karmon constant ≈ 0.4 (Stull, 1988):

$$\nu_t = (kz)^2 \frac{\partial \bar{\mathbf{u}}}{\partial z} \quad (2.9)$$

Then, equation 2.8 can be rewritten as:

$$\frac{\tau}{\rho} = \overline{\mathbf{u}'\mathbf{w}'} = -((kz)^2 \frac{\partial \bar{\mathbf{u}}}{\partial z}) \frac{\partial \bar{\mathbf{u}}}{\partial z} \quad (2.10)$$

This assumption is reasonable for a neutral atmosphere; but, once again it breaks down as the flow interacts with buildings and other objects, and in unstable atmospheres.

Another common way of generating an assumption for this mixing length is using the Monin-Obukov length, which calculates a characteristic turbulent transfer length using several atmospheric factors, also derived from dimensional analysis. There are many other parameterization techniques that are based on atmospheric conditions. However, for urban microscale modeling, we must use a technique that will be based more on local conditions rather than parameterization because we must deal with both atmospheric flow and flow around obstacles.

A popular approach for obtaining a closure equation involves the parameterization of a local characteristic mixing length by including generation and transport equations for two new scalars: the turbulent kinetic energy (TKE) and the dissipation rate of TKE, labeled ε . Intuitively, one can get a sense of dissipation rate by imagining a turbulent eddy moving through the flow carrying turbulent kinetic energy. The distance that an eddy will travel before degrading into heat and lots of smaller eddies will be determined by the rate of dissipation, ε , of the TKE. The equation relating these two variables is known as the standard K- ε model and is the most widely used turbulence closure model in CFD. Since ε has the dimension inverse time, if we are to maintain the dimensionality of ν_t (see Equation 2.9) the relationship between TKE and ε will be:

$$\nu_t = C_\mu \frac{K^2}{\varepsilon} \quad (2.11)$$

where C_μ is a dimensionless constant, K is TKE, and ε is the dissipation rate of TKE.

The K- ε model introduces two new equations, one for turbulent kinetic energy production (from shear and buoyancy) and one for turbulent kinetic energy dissipation. Together they describe TKE transport. The production term will be discussed below in describing variations on the K- ε model, but this chapter will not explore the mathematics of these two equations. They are described in detail in several sources in the literature (e.g., Duynkerke, 1987; Richards and Hoxey, 1993).

With this K- ε model, we now have 4 equations and 4 unknowns that can be solved with boundary conditions applied:

- 4 unknowns: u , v , K , and ε
- 4 equations: conservation of mass, conservation of momentum, conservation of K , and conservation of ε

Because we have assumed the vertical pressure gradients are small in our local scale, P is not a variable; but, if it is to be included, the ideal gas law ($PV = nRT$) quickly provides an additional equation with no additional unknowns. Decomposing u and counting w , the vertical velocity, gives us six equations with six unknowns.

A variety of turbulence closure methods are available in most commercial CFD codes today. The most widely used for industrial applications is the standard K- ε model and variations of it (ERCOFTAC, 2000). However, the standard K- ε model has been found to be inadequate for computational wind engineering and only the K- ε variant models that have corrections for TKE generation/dissipation have shown reasonable results (Castro, 2003). This is generally due to over-predicting the eddy viscosity when the flow is highly rotational. The better performing variants of the K- ε model usually have terms that suppress the generation of TKE in regions of high vorticity (Murakami, 1998).

Besides the K- ε model and its variants, other closure models are also used in CFD. The K- ε and other major closure models used for atmospheric applications are listed in Table 1, which provides a simple description of each model. The estimate of computing power required is based on a typical small-scale modeling project of dilution of a plume around several buildings. The larger the size of the domain and accuracy needed, the more resolution would be needed in the model, and the more computing power would be needed. Modeling an entire city skyline with a modified K- ε model would require significant computing resources; it would also be inappropriate, as the scale would significantly exceed the region of validity of our assumptions.

Table 1. Various Turbulence Closure Models Used in CFD.

CFD Turbulence Closure Model	Method of Modeling Reynold's Stresses	Accuracy for environmental modeling	Use history	Computing Power required
Standard K- ϵ	Eddy viscosity parameterization	Problems with flow around bluff bodies: overproduction of TKE at sharp edges	Common earlier	Minimal: Standard PC
Variant K- ϵ	Eddy viscosity parameterization: correction term for TKE production/ dissipation	Better accuracy than standard K- ϵ for various aspects of the flow. Problems still inherent.	Most common now	Minimal: Standard PC
Reynold's stress models (RSM)	Direct modeling of parameterized Reynold's stresses	Proven better accuracy than K- ϵ but not as good as LES on average.	Rare	Substantial: Parallel multiprocessor
Large Eddy Simulation (LES)	Large turbulent eddies modeled in incoming atmosphere - subgrid scale turbulence only parameterized	Best accuracy	Increasingly common use	Substantial: Fast parallel multiprocessor
Direct Numerical Simulation (DNS)	No parameterization of turbulence	Good accuracy	Extremely rare: only simple cases	Enormous: Large mainframe

More sophisticated turbulence modeling schemes include Reynold's stress models (RSMs) and Large-Eddy Simulation (LES). RSM is similar to K- ϵ in the sense that it uses extra equations that describe the production and transport of turbulence. However, instead of parameterized TKE, RSM models use separate equations for each separate Reynold's stress. LES works by parameterization of the local-scale (subgrid) turbulence and full representation of turbulence greater than the grid size. Therefore, LES is best used for unsteady state solutions.

The general trend, as one would expect, is that the more sophisticated the model, the greater accuracy it has when used for atmospheric flows. More in depth discussion of the various models and variants is provided in the following section.

2.4 CFD Models

The simplest closure scheme that can handle both atmospheric flow and flow around bluff (i.e., non-aerodynamic) bodies is the standard K- ϵ model. It has been the work-horse of the industry, despite its drawbacks. Validation efforts have demonstrated the model's weakness in simulating flow around simple shapes (bluff body modeling). Thus, many modeling projects today use variants of the K-

ε model. Though dynamic LES will eventually be the preferred method as computational resources increase, variant K- ε models will continue to be the favored tool for many more years.

For computational wind engineering, much of the attention of model validation and verification has been focused on flow around bluff bodies. The performance of a model is often rated by its ability to match its predictions of flow around a simple bluff body to the results of wind-tunnel tests. Flow around a simple cube is the common experiment used in validation. The simplified “flow around a cube” case is ideal because, even though the shape is simple, the flow around the shape is characterized by complex flow structures such as vortices, separation points, and unsteady flux of turbulence zones. Figure 3 offers a simple illustration of the typical re-circulation zones around a cube. Our discussion of these models will refer to this validation exercise because it has been the benchmark test for comparison of models.

2.4.1 Standard K- ε Model

The standard K- ε model has been the most common turbulence closure model used in the past due to its robustness and computational efficiency in a variety of applications. It has validated well for various applications, but it has had problems in computational wind engineering. The main problem that much of the literature discusses is its difficulty with predicting the flow at the sharp edges of bluff bodies, particularly at the sharp roof edge of a block building. It is reported that this is due to overproduction of turbulent kinetic energy in regions of stagnant flow (Franke et al., 2004b; Tsuchiya et al., 1996).

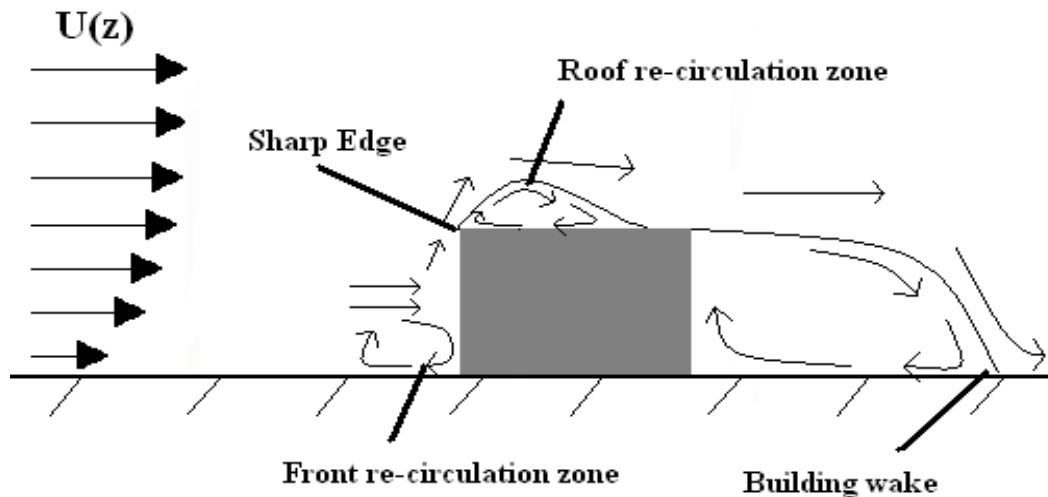


Figure 3. Illustration of the typical two-dimensional flow zones around a cube. Validation efforts using flow around a cube will involve comparing the qualities of these zones to physical tests.

This results in the model giving “mediocre” comparative results in areas of high anisotropy (Kim and Boysan, 1999). Generally, on a building, these areas are at the roof edge, in the wake at the windward edge of the building, and in the wake behind the building. Over/under predictions of TKE will travel downwind until dissipated, affecting the generation of TKE at points downwind, and resulting in errors in the dimensions of wakes and other flow features.

There are several modified K- ϵ model variants available. These variant models focus on changing aspects of the TKE, ϵ , and/or the constant C_μ (described below), to improve the predictability of turbulent viscosity at stagnant points in the flow. These models are, in essence, “ad hoc” for wind engineering. The changes limit the universality of the K- ϵ model, so what is good for bluff body flows might reduce the predictability of the model in other applications. And, even within bluff body studies, while they improve certain aspects of a flow description, they tend to worsen other aspects of the flow, leading to the conclusion that “ad hoc” models may not be the long-term solution for computational wind engineering (Easom, 2000). Nevertheless, these models do seem to perform better overall than the standard K- ϵ model. However, no matter how sophisticated the modified model is, the K- ϵ model is inherently limited by its assumption of isotropic eddy viscosity.

2.4.2 LK K- ϵ Model

The LK K- ϵ model (Kato and Laufer, 1993) was one of the early attempts to make an adjustment for the production of turbulent kinetic energy to coincide with vorticity of the flow. The model was developed strictly for bluff body flows to account for overproduction of TKE at sharp building edges. The production term for TKE in the standard K- ϵ model is:

$$P_k = \nu_t S^2 \quad (2.12)$$

where S is a scalar term related to the strain rate in the fluid. The LK model replaces this with:

$$P_k = \nu_t S \Omega \quad (2.13)$$

where Ω is vorticity. In simple shear flows, $\Omega \approx S$, and in stagnation regions $\Omega \approx 0$, so that the erroneous TKE production is limited in the vortex.

Lakehal and Rodi (1997) compared flows past a surface mounted cube modeled with the standard K- ϵ model and experimental results. They found improvement in the location and magnitude of the roof recirculation zone, and turbulent kinetic energy maxima. However, they noted that the model had poorer performance for the length of the re-circulation zone behind the block. The improved roof wake zone and longer building wake zones were also observed by Tominaga and Mochida (1999) using the LK model.

With less production of TKE at the building roof edge, less TKE advects into the building wake, which may account for the longer wakes. With higher TKE, vortexes would tend to dissipate more quickly. It was noted that vortex shedding behind the building contributes greatly to momentum exchange in the wake, leading to a smaller recirculation zone. The steady-state models cannot account for vortex shedding (Lakehal and Rodi, 1997).

2.4.3 MMK K- ε Model

The Murakami, Mochida, and Kondo (MMK) model is another example of ad-hoc models designed to improve the performance of the K- ε model for bluff body flows. The model itself is based on assumptions similar to the LK model, that is, that the production of TKE can be modified based on an observation of vorticity and strain at discrete points in the domain (Tsuchiya et al., 1996).

The author's approach with the MMK model begins by examining an inconsistency in the LK model - the production term of TKE is modified, but the loss of momentum to TKE term in the energy equation is not modified. Therefore, P_k in the TKE equation and P_k in the mean flow energy equation do not have the same form. Tsuchiya's approach is to deal with the eddy viscosity directly rather than tamper with the production of TKE.

The production term of TKE is dependent on the eddy viscosity:

$$P_k = \nu_t S^2 \quad (2.14)$$

Keeping the eddy viscosity equation in mind (Equation 2.11):

$$\nu_t = C_\mu \frac{K^2}{\varepsilon} \quad (2.15)$$

We see that we can alter the production of TKE by defining values of C_μ based on flow properties. The MMK model includes terms that define C_μ by the ratio of vorticity to strain rate:

$$C_\mu = C_\mu \Omega/S \text{ when } (\Omega/S < 1) \quad (2.16)$$

$$C_\mu = C_\mu \text{ when } (\Omega/S \geq 1) \quad (2.17)$$

Similarly to the LK model, TKE production will be limited when the Ω/S is low, such as in stagnant areas or centers of vortexes where the standard K- ε model has problems.

The authors note that the MMK model predicted the location and magnitude of the TKE maxima on the building roof better than the LK model did when

compared to the experiment. Also, the direction and magnitude of velocity vectors within the roof re-circulation zone were closer to the experiment than those calculated by the LK model. Other validation attempts have shown that the MMK model still over-predicts the length of the re-circulation zone behind the building (Easom, 2000).

2.4.4 Chen-Kim $K-\epsilon$ Model

The Chen-Kim model (Chen and Kim, 1987) is less of an ad-hoc model than the MMK model, but it is based on a similar assumption that production/dissipation of TKE can be altered to limit excessive TKE in regions of high vorticity. The Chen-Kim model contains a correction of the TKE equation by introducing a second time-scale of TKE production and dissipation dependent on the strain rate of the flow.

In general, the production rate of TKE is the product of turbulent viscosity and the strain rate of the flow. Chen and Kim argue that for rapidly evolving flow, such as in recirculation zones around bluff bodies, it is appropriate to restrain full production of the TKE to ensure that the energy generation rate is more realistic. They introduce two new time scales: the production time scale TKE/Pr_{TKE} and dissipation time scale TKE/ϵ . These two time scales are used in the expression for energy transfer rate from large scale turbulence to small scale turbulence in the dissipation equation. The inclusion of these terms enhances the development of dissipation rate, ϵ , when the mean strain rate is strong and suppresses it when the strain rate is weak. This allows the dissipation rate to respond more rapidly to control TKE development more effectively.

Chen and Kim compare modeling results of their alteration to the standard model for a number of common CFD validation exercises. The most applicable demonstration to our application is the flow over a backward facing step. The Chen-Kim model demonstrates superior performance in predicting reattachment length, surface pressures, velocity distributions, and turbulent kinetic energy magnitude and position when compared to the standard model.

Several studies are available in the literature that used the Chen-Kim model with varying success. One of these studies is Delauney (1996), who used the model for dispersion at an urban site and reported satisfactory results when compared to field data measurement of concentrations at the site. Delauney also conducted a validation exercise of flow around buildings and compared the standard $K-\epsilon$ model to the Chen-Kim model. He found overproduction of TKE in the standard model. He also reports the Chen-Kim model performed similar to the RNG model in the same comparison.

2.4.5 RNG K- ϵ Model

The Randomized Normal Group (RNG) K- ϵ model was developed based on RNG theory. RNG theory is a highly complex mathematical technique used to predict universal properties in distributions of chaotic phenomena such as turbulence. It originated in statistical physics and was used originally in quantum field theory (Kantha, 2000). It was first used in fluid turbulence to study fluctuations in a randomly stirred fluid at rest. Yakhot and Orszag (1986) were the first to use RNG to obtain equations and constants for fluid motion. The RNG K- ϵ model is identical to the standard K- ϵ model, except with an added term in the ϵ equation that limits the production of ϵ in areas of stagnation with rapid strain (areas of swirl). The model also uses revised constants. In this respect, the RNG model is similar in approach to the Chen-Kim model.

For simple flow around cubes and rectangular bluff bodies, the RNG model has shown superior performance compared to the standard K- ϵ model, more accurately predicting pressure distribution, TKE distribution, and flow (Kim, 1999). For flow over terrain, the RNG model has also been demonstrated to model flow and re-circulation better than other modified K- ϵ models (Kim and Patel, 2000).

There seems to be an overall consensus that the RNG model provides more accurate results (Franke et al., 2004b). However, the RNG model can be much more computationally expensive than other K- ϵ model variants, so its current use is still limited.

2.4.6 Reynold's Stress Models

Reynold's stress models (RSMs) are quite different in their approach to parameterizing turbulence. RSM uses the Navier Stokes equations and separate transport equations for each of the individual directional Reynold's stresses. This type of model will be quite useful for air quality analysis at the surface because it has the ability to incorporate the inherent anisotropy of the turbulence resulting from a boundary on one side (e.g., the earth's surface) and essentially unbounded flows on the other. However, the extra transport equations make this model much more computationally intensive than the standard K- ϵ model or its variants.

Although RSMs seemingly have a lot of promise, they have not been used extensively in computational wind engineering studies, most likely because of the added computational expense (Kim and Boysan, 1999). Some studies involving flow around a cube indicate that they perform with similar accuracy as the RNG model with only limited additional benefit. RSMs do show much promise for the future of computational wind engineering once the method is improved and larger, faster computers are more generally available (Easom, 2000).

2.4.8 Large-Eddy Simulation

Large-Eddy Simulation (LES) modeling is definitely the future of computational wind engineering as computer power increases and the modeling technique itself improves. LES has shown superior performance compared to all RANS modeling techniques. LES operates by parameterizing subgrid scale turbulence and by directly modeling the turbulence of larger scales. It is an unsteady state approach and is quite computationally intensive. More exquisite definition of the atmospheric boundary layer is needed since turbulence is directly modeled instead of parameterized by a TKE profile.

There is a temptation to use LES modeling over a larger scale than we are discussing in this chapter. When the scale of the domain is large enough that there is significant turning of the boundary layer due to Coriolis forces, the modeling must change fundamentally, as the atmosphere becomes distinctly nonlinear. When the basic assumptions used in deriving the Navier-Stokes equations no longer hold, the model cannot be expected to yield useful results. An alternative is an approach which models the atmosphere as organized large-eddies, developed by Brown (1991).

This chapter does not discuss LES in detail. The reader can refer to Chapter 5B of this volume for a detailed description of LES modeling of the atmospheric boundary layer.

2.5 Numerical Methods

One of the prime factors that led to the growth in the use of CFD is increased computational efficiency with the development of improved methods of solving the associated differential equations. Interestingly, some introductions to CFD focus almost entirely on these mathematical aspects, giving little attention to the physics.

For incompressible flow, which is what most civil engineering applications are concerned with, the Navier-Stokes equation and the mass continuity equation can be summed up as a relation between pressure and momentum, since velocity is dependent on the pressure gradient. Numerical schemes have been developed to solve the equations iteratively, known as pressure-velocity coupling schemes. In most commercial CFD codes, a variety of schemes are provided that the user can select. Most papers will report which pressure-velocity coupling method is used for their CFD project.

The two most popular methods are the Semi-Implicit Method for Pressure Linked Equations (SIMPLE) method and the Pressure Implicit with Splitting of Operators (PISO) method. There are several variants of the SIMPLE method also that are quite popular.

The SIMPLE method is a four stage process which involves a ‘guess, check, correction’ technique to solve the equations. The first step is to solve the momentum equation using the current pressure gradient computed from the last time step or initialization. It is highly unlikely that the first step generated velocity field will satisfy the conservation of mass and momentum. Next, pressure changes are estimated based on the new velocity. The SIMPLE approximation at this point is to assume that the velocity is dependent only on the pressure gradient across the cell, and ignore mass flux out of the cell faces. Third, the velocity is again adjusted to account for mass continuity. Fourth, the solution is repeated until the solution converges (Apsley, 2003).

There are several variants to SIMPLE that attempt to account for some of the weaknesses of the approach. In SIMPLE, it has been observed that correction equations are good for updating velocity, but not pressure since significant terms are ignored in the approximation of the pressure-velocity link. The variant SIMPLER is formulated to account for this by adding an additional equation for pressure used before the pressure-correction step. SIMPLEC is a variant that accounts for the velocities at the cell faces, rather than ignoring them as in the SIMPLE approximation.

The PISO method is other important type of pressure-velocity coupling scheme. It is similar to SIMPLE in many respects. However, it takes a different approach at estimating pressure and velocity, based on the surrounding flow properties rather than through steps of iteration.

The first few steps of PISO are essentially the same as SIMPLE, but with forward time marching. A solution to the velocity field is estimated by one time step forward and the pressure gradient and density is corrected to account for mass continuity. Instead of iteration, the PISO method takes into account conditions at neighboring cells from the time marching advection (Adaptive Research, 1997).

The general industry consensus is that a more advanced method than SIMPLE such as the SIMPLE variations or PISO should be used. This will not necessarily improve accuracy, but it may improve convergence behavior and lower numerical diffusion. In terms of model convergence performance, Jang et al. (1986) compared the performance of the SIMPLER, SIMPLEC, and PISO algorithms in a number of simplified CFD cases. The cases included expanding flow in a channel, swirling flow with scalar transport, and convection due to a heated wall in an enclosure. In general, no real advantage of using SIMPLER versus SIMPLEC is observed. The SIMPLEC algorithm tends to converge slightly faster than the SIMPLER method in some cases. PISO performs better than the SIMPLE derivatives in terms of quicker convergence at larger time steps with less computing effort in isothermal conditions. In the cases where temperature varies, the PISO algorithm converged slower and only at smaller time-steps than the SIMPLE variants.

2.5.1 Commercial CFD Codes

Computational Fluid Dynamics commercial packages usually consist of: 1) a solver program that performs the computations; 2) a graphical user interface where boundary conditions, mesh, and geometry are defined, and 3) a post-processor where the results are viewed in a graphical user interface. Most CFD solvers were originally developed by government laboratories and university research programs. Some of these have been developed into efficient graphical user interfaces.

Commercial CFD software packages are now available from many vendors. Most packages are general-purpose codes with various features. However, some application specific packages are available that are related to the environmental sciences. Application specific packages often contain the same features as the general-purpose package but with additional specialized boundary condition features. Specific applications range from aerospace engineering to electronic equipment cooling. Average cost for a commercial software license is about \$20,000 a year for the more popular packages. Several of the smaller firms offer packages for as low as \$3,000 - \$10,000 per year, which generally contain many of the same features as the more popular packages. For educational purposes, most firms offer substantial discounts and some firms offer limited-use student packages at very low prices.

The largest general-use CFD vendors are:

- Fluent[®] (www.fluent.com): Fluent general-purpose and application specific packages.
- CD-Adapco[®] (www.cd-adapco.com): Star-CFD general-purpose package.
- ANSYS-CFX[®] (www.ansys.com): CFX general-purpose package and application specific packages.

Some smaller CFD vendors offer packages that are often nearly equivalent in features and abilities to the larger vendors, at lower cost. These vendors include:

- Adaptive Research[®] (www.adaptive-research.com): CFD2000 general-purpose package
- CHAM[®] (www.cham.co.uk): PHOENICS general-purpose package

Several commercial vendors offer packages that have added features or adaptations for air quality applications at the local scale. The most popular of these are used more for indoor applications. They contain specialized boundary condition options for various HVAC equipments (e.g., diffusers, air conditioners, and heating apparatus). However, since these packages are geared towards building HVAC, they often do contain options for modeling the flow and air quality around the exterior of buildings. Two popular packages are:

- *Airpak*[®] from Fluent[®] (<http://www.fluent.com/software/airpak/index.htm>)
- Flovent[®] from Flomerics[®] (<http://www.flomerics.com/flovent>)

There are few commercial CFD packages that are custom-made for small-scale atmospheric environmental modeling. These models generally include the same functions as a general-purpose commercial CFD package, but with tools that allow easier topography definition, AutoCAD[®] import for building design, and wind data from meteorological files. The actual mathematics and turbulence models within the solver are no different from what can be found in a general-purpose package, usually utilizing the same standard K- ϵ or modified K- ϵ models.

Panache[®] from Fluidyn (www.fluidyn.com) is a CFD package for atmospheric dispersion, which is pre-packaged with several different turbulence models and a handy meteorological data input scheme. Surface wind data can be prescribed at different points in the domain for better initialization. Panache contains a standard K- ϵ model, as well as two one-equation models: a K-diff model that uses Monin-Obukov similarity for flow over flat terrain, and an LK model that can simulate different atmospheric stabilities. This model is even referenced by the EPA as an alternative to the official EPA dispersion models (www.epa.gov/ttn/scram001/dispersion_alt.htm).

Another commercial package is CFD-Urban developed by CFD Research Corporation (www.cfdrc.com). It was derived from the commercial CFD package CFD-ACE+, also from CFDRC. The model has the ability to use both LES and RANS turbulence models. The model has been validated against several field studies using the RNG K- ϵ model (Coirier, 2004), including the MUST, Kit Fox, and Prairie Grass dispersion field experiments.

Another is the FLACS-dispersion CFD model. The FLACS suite of models is developed by GexCon (www.gexcon.com), and is primarily used as an explosion simulator. The dispersion CFD model has been extensively validated and contains several features handy for atmospheric simulation - easy CAD import, and a “wind” boundary condition that maintains a wind and turbulence profile.

A number of urban dispersion simulators have also been developed by various government institutions. FEFLO, FAST3D, HIGRAD, and FEM3MP are several models that were developed primarily for military purposes. The high level of attention paid to terrorist attacks has driven the interest to accurately model the dispersion of chemicals in an urban area. FEFLO and FAST3D are Department of Defense models. FEM3MP is the Department of Energy model. HIGRAD is the model developed by the Los Alamos National Laboratory. All of these models are generally run as LES models, but some provide variant K- ϵ models. These models are actively being used in field studies such as the Urban2003 and Urban2000 studies, where tracer gases are released in urban areas in the United States to collect data for model verification.

Air quality modeling for regulatory purposes in the United States is generally the domain of the Environmental Protection Agency (EPA). The EPA has not developed its own CFD model for small scale modeling, but is actively exploring

the use of CFD for the future. Alan Huber's group at the EPA National Exposure Research Laboratory has been doing some work attempting to develop a method to use CFD for small-scale air quality studies. The work so far has generally focused on validation efforts, attempting to find the best way to simulate the atmosphere using the Fluent commercial software CFD package (Huber et al., 2004). Recent work has involved a comparison of CFD simulations to the Project Prairie Grass field experiment. This experiment was one of the main studies used to determine the properties of plume dispersion during different atmospheric conditions, giving rise to the Pasquill-Gifford stabilities and dispersion curves. They have found good agreement between the CFD simulations and the experimental data (Tang et al., 2005).

Additional detailed information on these and other CFD modeling codes, as well as links to a wide variety of the latest research, can be found on the portal website, www.cfd-online.com.

3 Simulating the Atmosphere in CFD

The EPA Guideline for fluid modeling of atmospheric dispersion (Snyder, 1981) provides guidance on atmospheric simulation that can be used for CFD studies. The guideline is intended mostly for wind tunnel modeling, and therefore, primarily discusses scaling.

An advantage of using CFD is that no scaling is necessary since the exact dimensions of the experiment can be represented in the computational domain. The important details in the Guideline for simulating the dispersion of exhaust around a building, not related to scaling, can be summarized as:

- The flow must be fully turbulent. This is ideal for RANS modeling, since the TKE is parameterized.
- The Coriolis force can be ignored at such a small scale (about 1 km).
- The incoming flow should be horizontally homogeneous, which will not be the case at larger scales.
- A logarithmic wind profile extending to the height of the boundary layer is needed, dependent on the friction element height, z_o .
- Turbulence intensity, which decreases with height, and background turbulence must be simulated.

The wind and turbulence profiles are crucial for dispersion modeling because they influence the size and location of flow characteristics around buildings. Also, the rate and direction of dispersion is highly dependent on the wind and turbulence profile. Early wind tunnel modeling demonstrated that plume spread and recirculation zones around buildings vary greatly depending on the characteristic profiles.

In non-steady state CFD modeling such as LES modeling, dynamic boundary conditions would need to be established for the modeling effort. The incoming wind would need to represent the actual atmosphere with incoming turbulent eddies appropriate to those generated by the general upstream land characteristics under the atmospheric conditions being simulated. Again, at scales approaching 10 km, the incoming turbulent eddies begin to be better defined as organized large eddies, which even LES cannot handle.

This chapter primarily deals with a steady-state solution used in RANS modeling. With a steady-state solution, the atmospheric wind profiles and turbulence profiles can be defined with no actual rolling vortices or other structures of turbulence. Turbulence is parameterized as TKE, and in a steady state solution, the wind profile can simply be represented by the mean wind profile of the atmosphere.

3.1 Steady-State Approach Flow

In the surface layer of the atmosphere, a number of characteristics of the atmosphere can be ignored and some assumptions can be made if we are going to be modeling airflow at a micrometeorological scale.

Pressure can be assumed to be constant. The top of the modeling domain will generally be lower than 200 meters (Richards and Hoxey, 1993), which is about a 25 mb pressure difference in a standard atmosphere from surface to top of the domain. The atmosphere can be assumed to be hydrostatic as the pressure force upward is balanced by the gravitational force downward, so that the vertical pressure field is irrelevant. In this respect, gravity can be ignored. Buoyancy forces can be simulated using a Bousinessq assumption that simulates buoyancy simply as a function of temperature difference. Also, the scale must be kept small enough that the Coriolis force can be ignored.

A commonly accepted set of boundary conditions for the K- ϵ model is described by Richards and Hoxey (1993). Assuming a steady state equilibrium boundary layer, the incoming atmosphere can be described by a profile of wind speed, TKE, and dissipation rate of TKE. The derivation of these is described in Easom (2000).

The Harris and Deaves (1981) model states that the wind profile of the atmospheric boundary layer, $U(z)$, can be described by a logarithmic equation dependent on friction velocity (u_*) and the depth of the surface layer (δ), where κ is the Von Karmon constant (~ 0.41), z height above the surface, and z_o the surface roughness length:

$$U(z) = \frac{u_*}{\kappa} \left[\ln \left(\frac{z + z_o}{z_o} \right) + 5.75 \frac{z}{\delta} \right] \quad (3.1)$$

The friction velocity, u_* , can be estimated from this equation if the surface roughness length, z_o , and the windspeed at a reference height are known:

$$u_* = \frac{\kappa U_{ref}}{\ln\left(\frac{z_{ref}}{z_o}\right)} \quad (3.2)$$

Assuming that in the equilibrium boundary layer shear stress decreases with height, an expression can be derived for TKE, where C_μ is the turbulence constant.

$$TKE = \frac{u_*^2 \left(1 - \frac{z}{\delta}\right)^2}{\sqrt{C_\mu}} \quad (3.3)$$

The dissipation rate can be assumed to equal the rate of generation of TKE, which is described by the equation:

$$\varepsilon(z) = \text{generation of TKE} = \frac{\tau_z}{\rho} \frac{\partial u}{\partial z} \quad (3.4)$$

Using the derivative of the wind profile equation, an expression for dissipation can be resolved from the TKE generation equation:

$$\varepsilon(z) = u_*^2 \left[1 - \frac{z}{\delta}\right]^2 \frac{u_*}{\kappa(z+z_o)} \left[1 + 5.75 \frac{(z+z_o)}{\delta}\right] \quad (3.5)$$

The depth of the boundary layer can be estimated using the equation (Huser, 1997):

$$\delta = 0.4 \sqrt{\frac{u_* L}{f}} \quad (3.6)$$

where L is the Monin-Obukov length and f is the Coriolis parameter (0.000125/second). A typical L is 10^4 for neutral atmospheric conditions, and a typical neutral boundary layer depth may be 500 - 1500 meters.

Richards and Hoxey (1993) assumed that when modeling very near to the surface, as would be the case in urban microenvironment studies, the height variation is much smaller than the depth of the boundary layer ($z \ll \delta$) so that shear stress is virtually the same at the top and bottom of the modeling domain. With this assumption, the term $z/\delta \approx 0$ and our 3 equations now become:

$$\text{Wind Profile: } U(z) = \frac{u_*}{\kappa} \left[\ln \left(\frac{z + z_o}{z_o} \right) \right] \quad (3.7)$$

$$\text{TKE Profile: } K = \frac{u_*^2}{\sqrt{C_\mu}} \quad (3.8)$$

$$\text{TKE Dissipation Profile: } \varepsilon(z) = \frac{u_*^3}{\kappa(z + z_o)} \quad (3.9)$$

These equations for the steady-state wind and turbulence profiles can be used for the air inlet and initial conditions in the CFD domain. This is an advantageous set to use because all equations are simply dependent on friction velocity, estimated easily from Equation 3.2 if the roughness length is known. However, this may only be applicable to small-scale studies with short buildings because TKE will decrease with height above the surface layer. In that case, Equation 3.3 should be used for the TKE profile and Equation 3.5 for the dissipation rate profile.

3.2 Surface Roughness Lengths

With the wind and turbulence profiles determined by friction velocity, z_o is the most important parameter in the neutral boundary layer since the u_* equation is a function of z_o and U at a reference height. Values for z_o have been well documented by studies of wind profiles and friction element distributions in various geography and land use situations. Typical values for z_o are provided in Figure 10.5 of Arya (1988). A few of the entries from that figure are given in Table 2.

If the typical friction element height can be easily estimated for a region in question, the ratio between roughness length and friction element height can be useful in determining the surface roughness length for the region. Arya states that the ratio of the roughness length and the average friction element height (z_o/h_o) varies from 0.03-0.25, increasing gradually with rougher surfaces. For grasslands a typical value of z_o/h_o is 0.15.

Table 2. Typical Surface Roughness Lengths.

Terrain	Surface roughness length, z_o
Level grass plains	0.01
Farmland	0.1
Rural, few buildings	0.2
Centers of small towns	0.5
Centers of large towns	1.0

Grimmon and Oke (1999) derive a set of surface roughness lengths for varying urban densities that is useful for determining which z_o to use in an urban micrometeorological study. It includes various measurements and estimates of z_o and other aerodynamic properties from a database of studies. That paper includes a typical set of aerodynamic properties for varying urban densities. They are given in Table 3.

In Table 3, the surface roughness lengths provided are a range of values dependent on the density of vegetation. A city such as Phoenix, Arizona, with sparse vegetation, will have z_o near the lower end of the range. A city such as Seattle, Washington, with dense vegetation in urban areas, will have z_o near the upper end of the range. Grimmond and Oke also point out that sites with deciduous tree cover will have 20% - 30% smaller z_o values during the time of year with no leaves on the trees.

Table 3. Typical Urban Surface Roughness Lengths.

Urban surface form	Surface roughness length, z_o
Low height and density: Residential one and two story houses, mixed houses and small shops, or light industrial and warehouses	0.3 - 0.8
Medium height and density: Residential two and three story apartment buildings, shops, schools, churches, and light industry	0.7 - 1.5
Tall height and high density: Closely spaced <six story apartment buildings, universities, heavy industry, town center.	0.8 - 1.5
High-rise Urban core and dense urban surroundings.	> 2.0

As a general rule of thumb, the estimate that $z_o \sim 0.1 \bar{z}_h$ is generally valid. Grimmond and Oke explored several different methods of calculating z_o from literature, and compared the results of these methods to databases of observations. The ratio, z_o/\bar{z}_h , generally ranged around 0.1 for surface element densities found in real cities.

3.3 Urban Wind Profile Displacement Height

In a micrometeorological study using CFD, the local wind climate must be analyzed and wind scenarios must be selected to represent various meteorological conditions that may occur. Wind data are collected at surface meteorological

towers at airports, universities, agricultural sites, air quality observation sites, elementary schools and a variety of other locations. A graph known as a “wind-rose” can be developed from the annual data set of wind speed and direction to display observation frequencies.

Most meteorological surface data are purposely collected at locations clear of obstacles, such as trees and buildings, to ensure that local winds are representative of the wider area. Because of this, the nearest meteorological data set to the site of your micrometeorological study often will have wind speed data that is higher on average than that of the study site. The higher density of obstacles will slow the average wind speed. Meteorological datasets nearest to the study site should be selected so that wind direction is approximately the same. If the density of friction elements near the study site warrants it, a “displacement height” for the approach wind profile should be used. The displacement height is a “lifting” of the wind profile to a height above the surface determined by the influence of the obstacles at the site. It is used for the approach flow in a CFD study to account for the differences in wind profiles from the data collection site and the CFD study site.

The displacement height, z_d , is a function of the surface friction element average height, \bar{z}_h . The simplest approximation of displacement height has been the assumption that it is a linear relation to surface friction element height (Grimmond, 1999).

$$z_d = C_d \bar{z}_h \quad (3.10)$$

Measurements of C_d range from 0.64 in field crops to 0.8 in forests. Hanna and Chang (1992) suggest $C_d \sim 0.5$ in their review of urban dispersion parameters. Grimmond and Oke (1999) argue that C_d varies depending on the density, arrangement, and shape of the surface roughness elements.

In terms of density, as friction elements become more compact, there is less room for momentum to penetrate into the canopy and the flow begins to “skip”. Thus, in the case of high density, z_d approaches \bar{z}_h . This can be observed walking through an urban center on windy days as the flags atop buildings are outstretched in the strong winds while the surface remains relatively windless.

In terms of shape, Grimmond and Oke note that trees and buildings will have profoundly different influences on the mean flow, even if they are the same average height. Buildings are solid objects with sharp edges that cause flow separation and vortex shedding, whereas trees are porous and pliable to the wind. Arrangement of the surface roughness elements can also influence z_d as buildings are arranged in grids that provide more or less open area for wind passage depending on the direction of wind flow.

Grimmond and Oke (1999) analyze several different equations from the literature developed to determine z_d and they compare the equations' performance to observations. They note that z_d/\bar{z}_h increases with increasing density of friction elements for each method analyzed, and that each method provides reasonable estimates.

A simplified technique can be used to estimate z_d using the results of Grimmond and Oke's sensitivity analysis (from Figure 3 of Grimmond and Oke). This can be done by fitting a mean line through results of z_d/\bar{z}_h based on plan areal fraction (λ_p), where A_p is the area covered by buildings, trees, and other surface friction elements and A_t is the total area.

$$\lambda_p = \frac{A_p}{A_t} \quad (3.11)$$

$$C_d = \frac{z_d}{\bar{z}_h} = 0.2 + \lambda_p \quad (3.12)$$

Estimate λ_p from at least a $\frac{1}{2}$ mile upstream 30° sector of urban landform. These equations can be assumed to fit closely to the average C_d from the various methods analyzed in Grimmond and Oke for $0.1 < \lambda_p < 0.7$, which covers the range of most real cities.

Grimmond and Oke also include a table of typical displacement heights as observed in varying urban landscapes. These values are given in Table 4.

Table 4. Typical displacement heights.

Urban surface form	Displacement height, z_d
Low height and density: Residential one and two story houses, mixed houses and small shops, or light industrial and warehouses	2 - 4 m
Medium height and density: Residential two and three story apartment buildings, shops, schools, churches, and light industry	7 - 14 m
Tall height and high density: Closely spaced < six story apartment buildings, universities, heavy industry, town center.	11 - 20 m
High-rise: Urban core and dense urban surroundings.	> 20 m

In Table 4, the displacement heights provided are a range of values dependent on the density of vegetation. A city such as Phoenix, Arizona with sparse vegetation will have z_d near the lower end of the spectrum compared to a city such as Seattle, Washington with dense vegetation in urban areas.

The displacement height can be applied to the incoming wind-flow equation so that the wind profile is raised. Equation 3.7 is altered to account for the newly calculated displacement height. This is expressed in Equation 3.13, where δ is the displacement height:

$$U(z) = \frac{u_*}{\kappa} \left[\ln \left(\frac{z + z_o - \delta}{z_o} \right) \right] \quad (3.13)$$

The wind speed reference height, z_o , that is commonly at 10 meters (the common wind measurement height), is now displaced 10 meters above the displacement height. According to this new wind profile, the wind-speed approaches zero at the displacement height and it is undefined below the displacement height. Therefore, below the new wind reference height, the wind profile is no longer valid. We must apply another wind profile equation to account for wind from the surface up to 10 meters above the displacement height (if 10 meters is the original height of the wind reference).

We can calculate this wind profile using the logarithmic Equation 3.7 and a new friction velocity. Using the same z_o as measured for the above-displacement wind profile, a new, lower zone friction velocity can be calculated using Equation 3.14. This equation solves for the friction velocity by using the reference wind speed at its new height:

$$u_{* \text{ canopy}} = \frac{\kappa U_{(ref+\delta)}}{\ln \left(\frac{z_{(ref+\delta)}}{z_o} \right)} \quad (3.14)$$

The final incoming wind profile will contain two parts, as illustrated in Figure 4:

1. A wind profile extending from the displaced wind-speed reference height (usually 10 meters above the displacement height) to the top of the domain, determined from Equation 3.13.
2. A wind profile extending from the surface to the displaced wind-reference height using Equation 3.7, but using the friction velocity calculated from Equation 3.14.

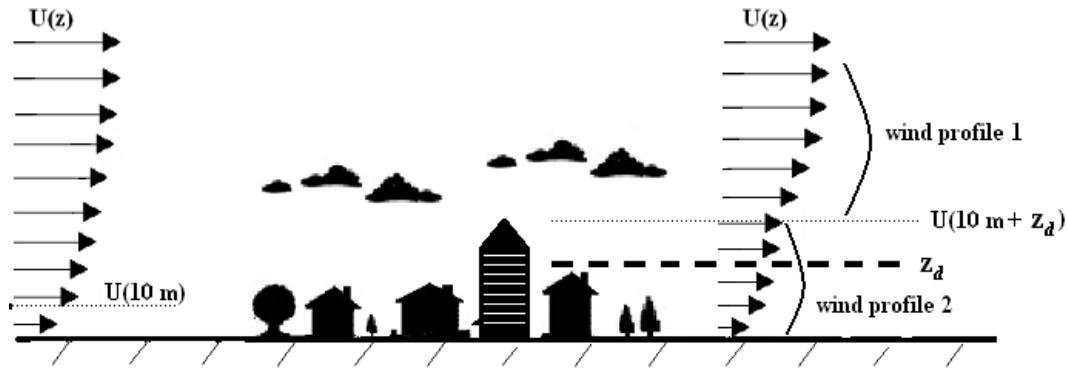


Figure 4. Illustration of the two wind profiles used if an urban displacement height of the main wind profile is necessary. Wind profile 1 uses the standard equation displaced upward by the displacement height. Wind profile 2 extends from the surface to the wind observation height: the displacement height + the wind observation height (usually 10m).

3.4 K- ϵ Constants

Richards and Hoxey (1993) argue that the standard K- ϵ modeling constants are not universally applicable and new constants must be determined to apply the model to the neutral atmospheric boundary layer. By analyzing the conservation equations of TKE and ϵ , they note that the boundary equations satisfy the conservation equation for ϵ only if:

$$\sigma_{\epsilon} = \frac{\kappa^2}{(C_2 - C_1)\sqrt{C_{\mu}}} \quad (3.15)$$

σ_{ϵ} , σ_K , C_2 , C_1 , and C_{μ} are the constants of the TKE and ϵ conservation equations that were originally estimated by Launder and Spalding (1974), and κ is the Von Karmon constant. Constant C_{μ} is the constant of proportionality that relates the turbulent viscosity to the length and time scales of TKE (from Equation 2.15). Constants σ_{ϵ} and σ_K are the turbulent Prandtl numbers for TKE dissipation and TKE, respectively. These constants relate the advection of TKE and ϵ through the atmosphere to the viscosity. Constants C_2 and C_1 are proportionalities that determine the production and loss of TKE dissipation rate.

The commonly used values for the constants are based on an evaluation of plane turbulent free jets and mixing layer simulations (Adaptive Research, 1997). They represent a “consensus” parameter set and can be assumed to represent a flow dependent model accuracy of 10-50%. The constants are:

$$\sigma_{\epsilon}= 1.3 \quad \sigma_K=1.0 \quad C_1= 1.44 \quad C_2= 1.92 \quad C_{\mu}= 0.09$$

where κ is the Von Karmon constant estimated to be about 0.433 to satisfy the equation with the Launder and Spalding constants.

While these constants are commonly used in general engineering applications of the K- ε model, they are not necessarily applicable to the atmospheric boundary layer. The description of atmospheric turbulence is highly dependent on the value of C_μ since it is directly related to the equation for viscosity. Constant σ_ε is, in turn, dependent on the value of C_μ as can be seen in Equation 3.7, but it has been shown that modeling results are insensitive to σ_ε (Bottema, 1997). Chen and Kim (1987) suggest that σ_K should be less than 1, recommending a value for σ_K of 0.75 to satisfy observations of ε dissipating lower in the boundary layer than TKE. C_1 and C_2 are evaluated in Deterling and Etling (1984) for use in the boundary layer and are taken to be 1.13 for C_1 and 1.90 for C_2 . These values are similar to Chen-Kim values of $C_1=1.15$ and $C_2=1.9$. Huser et al. (2000) suggest the use of $C_2=1.83$ to limit the destruction of ε to conform to observed phenomena.

It is likely that C_μ is observed to be lower in the atmospheric boundary layer flows due to “inactive” turbulence (Bottema, 1997). Inactive turbulence can be defined as the large eddies in the flow that contain a significant amount of the turbulent kinetic energy but do not actively represent Reynold’s stresses at the grid scale that is being modeled. That is, they are considered turbulent but are not as fully active in local turbulent mixing as smaller eddies. These large eddies are produced by gravity waves, flow over objects, convective cells and other atmospheric phenomena. The representation of TKE as a scalar is the main culprit in this problem – an inability to account for the size spectra of eddies and directional qualities of TKE in eddies.

To account for the inactive turbulence, C_μ must be altered. Richards and Hoxey (1993) observed that with the commonly used C_μ of 0.09, Equation 3.8 gives K/u_*^2 as 3.3 in the surface layer of the neutral atmosphere. They further observed that the data from five different studies of the surface layer suggest a K/u_*^2 value greater than 3.3. Table 5 shows the values of K/u_*^2 from those studies and the calculated values of the constants C_μ (from equation 3.8) and σ_ε (from equation 3.15).

Table 5. K/u_*^2 Observed Values and Corresponding Calculated Constants.

Study	K/u_*^2	C_μ	σ_ε
Klebanoff (1955)	3.35	0.089	1.23
Panofsky & Dutton (1984)	5.48	0.033	2.02
Hagen et al. (1981)	6.2	0.026	2.28
ESDU (1985)	7.26	0.019	2.67
Silsoe (Richards and Hoxey, 1993)	8.75	0.013	3.22

Table 5 supports the value of 0.03 for C_μ estimated by Bottema (1997). However, such a low value for C_μ may only be appropriate in some portions of an urban

modeling domain. In a typical flow around a cubical building, several re-circulation zones will occur, as illustrated in Figure 3. The large re-circulation zone at the roof of the building and in the wake of the building will contain a large amount of turbulent kinetic energy, most of which is stored in larger eddies. In these regions, a lower value of C_μ may be justified. This suggests that different C_μ values may be needed within one domain, varied by the characteristics of a zone. Bottema (1997) recognized this by examining the roughness sublayer that is typically above the layer of buildings at the surface. Above the obstacle tops, inactive turbulence becomes significantly less, justifying a higher C_μ value. Varying the C_μ value is a feature of the Realizable K- ϵ variant model, with a resulting improved performance over the standard K- ϵ model.

Based on these papers, a set of constants for the K- ϵ model and its variants in the neutral boundary layer can be recommended:

$$\sigma_\epsilon = 2.12 \quad \sigma_K = 1.0 \quad C_1 = 1.15 \quad C_2 = 1.83 \quad C_\mu = 0.03$$

3.5 Domain Turbulence Distribution

One of the more important initial conditions that must be defined for a CFD model of the urban environment is an accurate wind and turbulence structure of the atmosphere. And this wind and turbulence structure must be maintained throughout the domain, except as it is modified by the structures and other blockages. However, it has been observed by many researchers (e.g., Hanna et al., 2004 and Riddle et al., 2004) that the TKE tends to dissipate too much in K- ϵ models, resulting in domain-exiting wind and TKE profiles that are not consistent with the incoming profiles, even in domains of consistent flat terrain.

It is a common recommendation, as described below, that CFD modelers conduct an initial model run in their domain with all internal obstacles temporarily removed. The results should confirm that the wind and turbulence profiles exit with almost the same profiles as the incoming air.

One approach to alleviate this problem has been suggested by Tang et al. (2005). A two-step approach involves initial modeling with a wind and turbulence profile estimate. The inlet and outlet of the model are coupled using “periodic” boundary conditions, which is part of most commercial CFD software packages. In this method, the outlet profile is used to iteratively modify the inlet profile until a stable boundary layer is obtained. Then, the user alters the mass flow into the domain until the desired friction velocity is achieved. From this process, profiles of velocity, TKE, and ϵ are calculated, which can be used as inlet conditions for the main modeling.

Another method to prevent TKE decay is to include a turbulence source term throughout the whole domain. From our observations with various projects, the TKE tends to dissipate fastest near the surface because of the higher initialized

dissipation rate of TKE at the surface. Our first attempt at a turbulence source term was to add a domain wide source term equal in rate to the dissipation term. However, this tended to overproduce TKE within the domain.

Through experimentation we have found that a turbulence source term of 60-80% of the TKE dissipation rate tends to help secure a constant wind profile and TKE profile in the domain. The coefficient will vary depending on the wind, turbulence magnitudes and choices for the K- ϵ model constants. This ad-hoc method is useful, but it should be noted that a domain wide source term will include production of TKE within areas of wind interaction with the structures and other boundary conditions within the domain. A possible alternative may be to contain the source region at the windward lead to the obstacles, ignoring the downwind region if dispersion of pollutants is unimportant there.

3.6 Pollutant Dispersion

Dispersion of pollutants in the atmosphere is due to advection, molecular diffusion, and turbulent diffusion. Molecular diffusion is irrelevant in the short time scales used in urban microenvironment studies. Advection of pollutants by wind will be fairly accurate if a proper wind profile has been prescribed and the flow patterns around the structures are improved by the use of a variant K- ϵ model or an advanced CFD model such as LES. Dispersion by advection can also be improved if modeling is conducted using an unsteady state model that allows for small time scale variances in wind speed and direction.

Turbulent diffusion is the primary process that determines pollutant dispersion in the atmospheric boundary layer. Therefore, when modeling dispersion, careful attention must be directed towards the parameterization of turbulence to obtain accuracy. Turbulent fluxes of momentum are not equal in all directions near the surface. In a stable and neutral atmosphere, turbulent flux in the vertical is less than that in the horizontal because the presence of the earth's surface and the wind velocity gradient tend to suppress vertical turbulence.

In a typical CFD study of the urban microenvironment, we are going to be interested in modeling the most common case, a neutrally stratified boundary layer. In this case, turbulence is entirely from mechanical forcing due to surface friction and vertical wind shear. Typical surface layer observations indicate that in neutral conditions, the three direction-dependent ratios are $\sigma_u/u_* \approx 2.5$, $\sigma_v/u_* \approx 1.9$, and $\sigma_w/u_* \approx 1.3$ (Arya, 1988). Considering these observations, it would be important to model dispersion based on independent, directionally-dependent turbulence parameters. Unfortunately, the standard K- ϵ model and most K- ϵ variants only consider turbulent kinetic energy as a directionally-independent scalar. A Reynold's Stress Model (RSM) would be a more appropriate model for dispersion modeling, since it is able to account for the individual, directionally-dependent Reynold's stresses (Riddle, 2004).

3.6.1 Diffusivity in the K- ϵ Model and Schmidt Numbers

When the K- ϵ model or K- ϵ variants are used, special approaches may be incorporated to account for the anisotropic turbulence of the actual environment. Tang et al. (2005) point out that the greater standard deviation of horizontal wind speed is due to turbulent dispersion and small changes in wind direction. To account for this, they modeled steady-state solutions and then smoothed the results over the expected range in wind direction.

Another option to simulate dispersion may be to modify the diffusivity of a pollutant in the vertical in order to restrict diffusion in the vertical. This can be done by assigning a higher Schmidt number to vertical diffusion than to horizontal diffusion. The Schmidt number is a coefficient that relates the turbulent viscosity to the diffusivity of a pollutant by the equation,

$$D = \frac{\nu_T}{Sc} \quad (3.16)$$

where D is the diffusivity of the pollutant, ν_T is the turbulent viscosity, and Sc is the Schmidt number. One would expect that in an atmosphere free of significant buoyancy forces, the diffusivity of a pollutant is entirely dependent on the diffusivity of momentum. With higher Schmidt numbers, the dispersion of the pollutant will be suppressed, or in other words, the pollutant will disperse slower than the diffusion of momentum. Typical dimensional Schmidt numbers may be $\sigma_y = 0.55$, $\sigma_x = 0.77$, and $\sigma_z = 0.77$, where z is vertical, x is with the flow, and y is perpendicular to the flow (Scanlon, 1997). Based on these values, a good base ratio of vertical dispersion to horizontal dispersion would be 5/7. These concepts are illustrated in Figure 5.

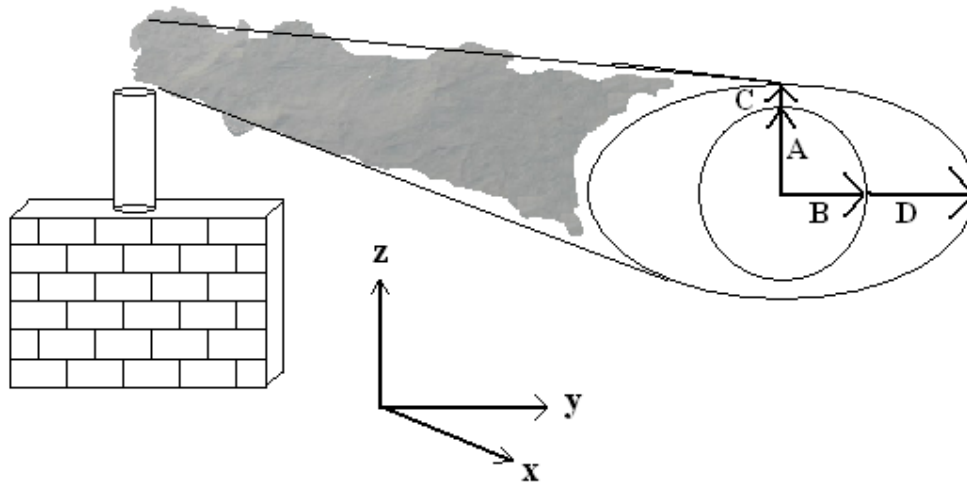


Figure 5. Illustration of the use of Schmidt numbers to parameterize dispersion. In this figure, a plume is dispersing downwind. The boundaries of the plume at a point downwind are illustrated in a vertical slice of the plume. Diffusivity of the plume is based on the turbulent diffusivity. Vertical spread A and horizontal spread B are equal in the case where no Schmidt number is used because turbulent diffusivity is not directionally dependent, being a non-dimensional scalar. Schmidt numbers can be applied (Equation 3.16) to enhance or limit dispersion in the x,y, or z direction to conform with realistic conditions. Spread C and D demonstrate the plume spread in the vertical and horizontal after different Schmidt numbers have been applied.

Some field studies and experiments have shown that the Schmidt number is fairly constant in the atmospheric boundary layer in the absence of significant buoyancy effects (Baik, 2003). So, the assumption of a constant Schmidt number may be valid for the general CFD case discussed in this chapter. Schmidt number values ranging from 0.18 to 1.34 have been measured in field observations under a variety of atmospheric conditions (Tang et al., 2006), but Schmidt numbers of 0.7 to 0.9 have traditionally been used in CFD models of the neutral atmosphere.

In a recent study, various Schmidt numbers were used in CFD simulations to compare with the Project Prairie Grass field dispersion study (Tang, 2006). CFD simulation results were compared to the plume centerline concentrations. In this study, the researchers found that a Schmidt number near 1.3 performed best for more near range dispersion (50 meters), and Schmidt number near 1.0 performed best for the longer range dispersion (100m – 800 m).

Based on the findings of the Tang et al. study, we recommend a higher Schmidt number than the typical range of 0.7 - 0.9 generally used in short range CFD studies. Values ranging from 1.0 - 1.3 would be more conservative numbers to use.

3.7 CFD Domain, Meshing, and Recommended Modeling Specifics

There is a consensus among urban wind engineering CFD researchers on certain aspects of the setup of the CFD domain and settings. The distance of the domain sides to the buildings, the resolution of cells within regions of interest, and the numerical settings of the model can all have significant influence on the quality of the modeling project. Recommendations for these settings are provided in this section.

3.7.1 Domain Size

It is important to ensure that the walls of the domain, which contain your inlet and outlet boundary conditions, are far from the subject buildings, sources, and significant topography. If they are too close, interactions between the boundaries can distort results.

In our earlier paper (McAlpine and Ruby, 2004) we provided a recommendation for domain size and the placement of buildings and obstructions in the domain that is based on air quality modeling rules. We have found that a rule based on the maximum modeled wind speed and building dimensions is effective in avoiding edge effects. Others have focused more specifically on the building height.

Hall (1997) recommends that the domain walls upwind of the building should be $5H$ in distance from the building with H being the height of the building. The top of the domain and sides of the domain should also be $5H$ in distance from the building faces or top. For multiple buildings, the height of each building needs to be taken into account to determine the distance as illustrated in Figure 6. Downwind, the outflow boundary should be at least $15H$ beyond from the buildings to allow the development of the flow behind the structures, which may extend some distance downwind (Franke et al., 2004).

If extensive topography is present in a model, it is advantageous to extend the domain boundary out to a region of relative flatness so that significant topographical features don't interact directly with the domain wall boundary conditions.

Buildings upwind of the site of interest need to be included in the modeling if they will have significant effects on the airflow at the site. This is especially true in high wind cases where significant "skipping flow" may occur. A general guideline is to include buildings upwind and downwind that are $6-10H_n$ in distance from the site of interest, where H_n is the height of the upwind/downwind buildings (Franke, 2004). For greater wind speeds, use the higher standard up to $10H_n$, and for lower windspeeds use $6H_n$.

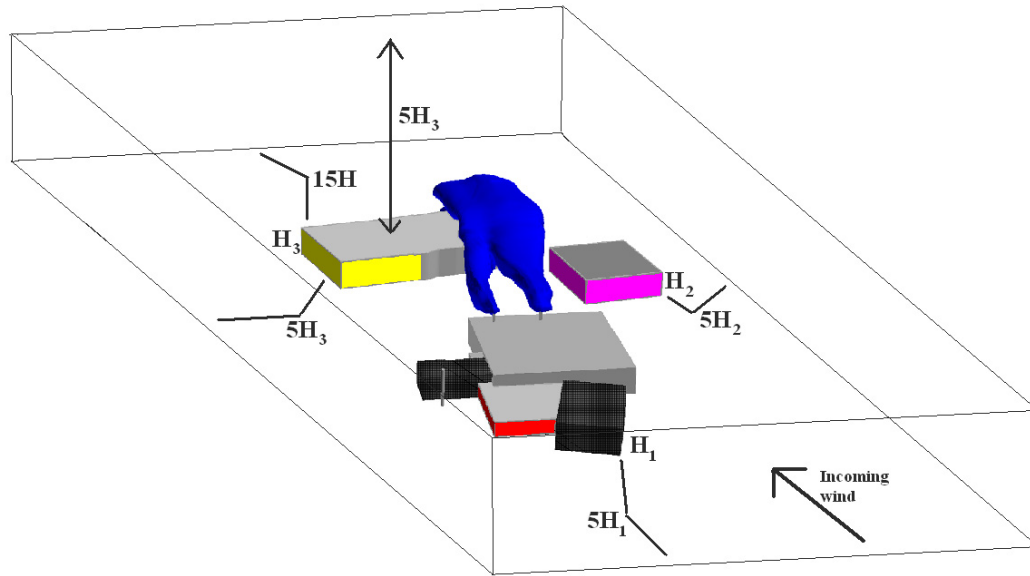


Figure 6. Illustration of domain wall distancing. The domain includes several buildings and one wind condition. Pollutants from two stacks are illustrated from the source building as blue plumes. H_1 , H_2 , and H_3 label the heights of the respective buildings.

3.7.2 Meshing and Cell Size

When building a model, careful attention needs to be directed towards determining the number of cells in the domain. With too few cells, the model may not be able to resolve the complex flow around objects or may result in excessive numerical diffusion. With too many cells, the computing resources may be limited, extending the time of model runs beyond the scope of your project.

A few sets of guidelines have been suggested for mesh sizing. Most of these are focused on structured hexagonal meshing of domains. Other types of meshing schemes may require other insight, but this does not mean they are not any better nor any worse than hexagonal meshing. Unstructured grids may be especially useful when grid refinement is needed near areas of concern or variability. However, the ERCOFTAC Best Practice Guidelines (ERCOFTAC, 2000) do recommend the use of hexagonal meshing over tetrahedral meshing when boundary layer modeling is critical.

The number of cells needed in the model can be estimated by the size of objects in the domain. One system of estimation is to include 10 cells per cube root of the building volume (Franke, 2004). For a cubical building of 10-meter sides, the building would have a volume of 1000 m^3 . The cube root of this is 10, so 100 cells per building side would be warranted. This is, of course, a vague guideline and would not be applicable to all scales.

Number of cells per unit length may be decreased further from the area of interest to limit the number of total cells in the domain. One recommendation is that the number of cells between buildings should be at least ten (Franke, 2004). Other minimum grid sizes suggested have been $0.025H$ (Cowen, 1997), $0.01H$ (Scaperdas, 2004), or $0.2H$ in the horizontal and $0.05H$ in the vertical (Bartizis, 2004).

There is relative flexibility in the number of cells chosen for a model. One must include enough cells to resolve the important flow features and site detail in the model. We have had some experience modeling large buildings with very small lab hood stacks. Our goal in these cases was to attempt to use 3 - 6 cells per smallest size of element so that the flow out of the stack would at least be partially resolved. If the element of importance, such as a small stack, is too small, then parameterization may be needed for pollutant release. One parameterization strategy may be using a "box model" that would define a zone around the stack outlet and modeling the flow and pollutant release from a specified distance from the stack. With a "box model", the correct volume and momentum of stack exhaust are modeled without the need of modeling the details of the stack itself.

Regardless of cell size, a mesh independence study must be conducted initially to get an idea of how the cell size influences the flow. Details such as TKE magnitude, recirculation zone location and size, or velocity magnitudes can be observed to judge mesh influence. The goal is to find the largest cell size that resolves the flow without significant changes from a slightly smaller cell size grid.

3.7.3 Modeling Time Steps

The length of time necessary for a steady-state solution in a micro-scale meteorological project will vary depending on the size of the domain and complexity of the model. A first-guess time estimate can be based on the 10-meter wind speed and the length of the model. For example, if your domain is 200 meters long and the wind speed is 4 m/s, then it would take 50 seconds for the incoming air to reach the other side of the domain in a flat, obstacle-free domain. This would be the first-guess minimum time and results every 5-10 seconds in a time series could be observed after 50 seconds until a steady state solution is qualitatively observed.

For most bluff body flows, a steady state solution may not be completely obtainable due to vortex shedding in the wakes of objects. For an air quality study, it is most desirable to try to use the set of results that most resembles the flow average. When observing an unsteady state solution, vortex shedding can be observed in the wake of the building. The solution can be frozen as a final result in the middle of a vortex shedding cycle so that the wake is near average size.

Overall, in our experience for typical flows of 2 m/s to 8 m/s in a domain size covering a city block or so, we tend to see a quasi-steady state solution around 100 - 200 seconds. We would recommend using at least a 90-second run for most typical modeling runs of this scale. After a steady state solution is obtained, it can be frozen and the model can be re-run with the species transport equation to model the dispersion of the pollutant throughout the domain.

3.7.4 Selection of Wind Scenarios for Modeling

When selecting the scenarios for modeling for a project, one needs to avoid redundancy and limit the number of runs. This is especially important for large complex domains where a single CFD run may take many days with desktop PC computing resources.

The most important wind directions are obviously those that blow directly from source to receptor. Receptors may include air intakes, operable windows, doorways, pedestrian walkways, and other sensitive locations where persons may be exposed to the contaminant. For each wind direction, a sensitivity analysis should be conducted by adjusting the wind direction by 3° - 7.5° clockwise and counterclockwise. The differences in concentrations at receptors should be noted for each alteration. A sensitivity analysis may also be needed even if your modeling approach includes an unsteady-state time averaged solution with incoming wind of varying wind directions.

For a pedestrian comfort or natural ventilation study, wind directions must be more uniformly distributed with perhaps a total of 16 wind directions analyzed to cover all the major wind directions (Ratcliff, 1990).

For wind speed, a good variety is needed to assess the distribution of mean wind speed and gusts. For pedestrian comfort studies, the higher wind speeds should be studied since high wind gusts will be the main cause of nuisance. For air pollution studies, lower magnitudes will need study since the most problematic situations occur when receptors are impacted for longer lengths of time.

Generally for air quality studies, the 99.5th percentile, 95th percentile, 75th percentile, and mean wind speeds for each wind direction are a good basis for wind speed selection. For example, for a meteorological data set in the Seattle area for a southwest wind, the 99.5th percentile is 9 m/s, 95th percentile is 6 m/s, 75th percentile is 3 m/s, and mean wind is 2 m/s. A good spread of wind speed is needed in a project to cover the variety of conditions that may occur. It is also advantageous to conduct a sensitivity analysis for a wind speed for each direction by varying the wind speed by 0.2 m/s or so.

4 Industry Opinion and Guidelines

Overall, the general opinion in the industry is that engineers and scientists should use caution in applying CFD to air quality questions. User skill continues to be an important element in model success. More validation work and continued improvement of turbulence models are needed. A number of guidelines and recommendations have been established to guide the practitioner, but they tend to differ from one another. This section reviews the current opinion of practitioners and outlines the various guidelines available at this time. The section concludes with a set of recommendations based on the available advice.

4.1 Industry Opinion

Much of the current opinion on the use of CFD is based on comparisons to physical modeling results, mainly wind-tunnel modeling. Reviewers admit that even though CFD has great promise in replacing the wind tunnel for micro-scale modeling, it is still in a learning stage. However, it is quickly maturing and its current use as an analysis tool is appropriate if used with caution and awareness of its weaknesses. Some of the complaints about CFD accuracy seem excessive and pedantic.

A review by Stathopoulos (1997) concluded that “practitioners should be warned about the uncertainties of the numerical wind tunnel results and urged to exercise caution in their utilization.” He is concerned that there is an “ever-increasing confidence in the results obtained by CFD codes and more and more papers propagate the idea that the numerical wind tunnel does exist today and produces results ready to be used by practitioners.” He reviews several of the more prominent current studies that compare CFD results to experimental data. He notes that while some results are quite good, others deviate greatly. Most of his criticism focuses on the poor pressure distribution on bluff bodies estimated by the standard K- ϵ model, which is widely acknowledged to be inadequate. For environmental flows and flow over complex terrain, the models perform better, but some problems are still evident. For air quality analysis projects, he again notes the poor performance of the standard K- ϵ model. An improved model better predicts the results in study he reviewed, with a tendency towards a conservative solution (over-prediction of pollutant concentration), which is beneficial for air quality planning.

In a review by Murakami (Murakami, 2002) of the CFD related research papers in the Computational Wind Engineering 2000 Symposium, he observes that, for his taste, the direction of research in the field is too focused on applications and not on improving the models themselves. He directs attention to the inadequacy of the log-law type wall boundary condition, the potential for high numerical error with the standard K- ϵ model, and the errors caused by poor modeler choice of gridding and boundary conditions.

While these authors note that “none of the existing models. . . [have] an overall high prediction accuracy”, “the prediction accuracy is sometimes insufficient” or the models “are not perfect”, they also observe “remarkable progress” in the development of CFD models. They note that “the predictions . . . are in good agreement with the experimental data.” They cite some papers with results in good agreement with the experimental data but also report a paper that “fails to predict” the experimental observations. Looking at each of the figures in the Stathopoulos paper, one can see close, but not precise, correspondence between the experimental data and the CFD results, with the range of CFD results similar to the spread in the experimental data.

Despite the acknowledged shortcomings of CFD modeling, there are some advantages to using it as an analysis tool. One benefit is that CFD can provide data at many more points than a wind tunnel and can work at full scale. This is a significant advantage over wind tunnels for urban dispersion (Wright, 2004), particularly when an area wide distribution of pollutant concentration is desired. The ability to model full scale allows for interactions between building interiors and exteriors, and in atmospheric boundary layers with various stability conditions, which is another advantage over a wind-tunnel.

Overall, the critics recommend that CFD be used as an analysis tool rather than a design tool in conjunction with another analysis method. Modeling might be conducted in conjunction with an alternative form of air quality analysis such as Gaussian modeling or theatrical fog release. In any case, careful scrutiny of the results is needed. Careful attention must be directed to the atmospheric boundary layer setup, preferably using a setup scheme and validation as suggested in this chapter. Any study should also include a grid independence run and sensitivity analysis of variations due to boundary conditions or wind speed and direction. Lastly, the shortcomings of the study should be communicated in the report.

4.2 Published Guidelines

There are several sets of CFD guidelines that can be applied to micro-scale urban air quality studies. In this section we will discuss the details of three distinct sets. It is recommended that any practitioner in the application of CFD for air quality analysis follow strictly the first of these sets (the ERCOFTAC set) of guidelines, and refer closely to the recommendations of the last two sets of guidelines (COST and QNET-CFD). An additional set of guidelines of best practice are presented in the Project EMU final report, which is based on the results of that study.

4.2.1 ERCOFTAC Guidelines

A set of best practice guidelines were published in 2000 for general use of CFD for industrial applications by the European Research Community on Flow, Turbulence and Combustion (ERCOFTAC, 2000). Practitioners frequently cite these guidelines as a foundation for industrial CFD practices. Though it is a

general set of guidelines, and does not contain any specific recommendations for computational wind engineering, it is a good basic protocol to follow for any CFD application.

The ERCOTAC guidelines were published by the Special Interest Group on “Quality and Trust in Industrial CFD.” They were commissioned following an “extensive consultation with European industry which revealed an urgent demand for such a document”. The guidelines claim that they offer about 20% of the most important general rules of advice and cover about 80% of applications. The content of the document is quite applicable to air quality studies considering the types of flows it focuses on. The majority of the document covers topics such as meshing, quality assurance, time-stepping, CFD settings, boundary conditions, and validation/verification.

Some of the more important guidelines from the document that can relate to most micro-scale air quality project are included here in an overview. Guidance for inlet/outlet and related boundary conditions for the atmosphere are not included, but the guidance recommends careful attention to the setup of these to correspond to the reality of the process being modeled. The setup procedures for the atmosphere discussed earlier in this paper generally comply with these guidelines.

One should obtain the document and follow its guidance if performing or reviewing a CFD project. Following is a discussion of a selection of the guideline’s topics that have not already been discussed in this paper:

- A. Validation - Guideline 11.5: “Validate it against test data for a similar application with similar flow structures and flow physics.”

Before beginning a CFD project, the user should conduct several sets of validation tests to establish the user’s ability and ability of the software to accurately model the type of problems being examined. This is important because it has been demonstrated that CFD project results can vary greatly from user to user simply due to personal choices for meshing and boundary condition setup, even using the same CFD code and prescribed conditions (Stathopoulos, 2002). Conducting the validation exercises is alone a valuable learning opportunity for the new CFD practitioner.

A good first validation exercise is to model the flow around a simple cube in an atmospheric boundary layer. A good set of data to use is that of velocity measurements from Minson (1995). Also, the lengths of re-circulation zones behind the block can be examined by comparing to those observed in wind tunnel tests conducted by Snyder (Snyder, 1994).

B. Model Choice - Guideline 11.6.1:

Be aware of the weaknesses of the standard K- ϵ model and use an alternative model if possible using the guidance this chapter has discussed. Conduct a sensitivity run by using a different model and comparing the results to your original model. For dispersion, a method must be used to account for the inability of the K- ϵ model to handle the anisotropy of turbulence in the surface layer of the atmosphere.

C. Guidelines on wall functions - Guideline 11.6.2:

Wall functions are used by CFD to parameterize the transition from laminar flow to turbulent flow at the wall boundary. The common log-law wall function calculates flow near a wall assuming that each cell is within the turbulent layer. Therefore, meshing must account for this, making sure that the center of the first cell is outside of the laminar layer. Not doing so can have an impact on the accuracy of the flow in terms of heat transfer and turbulence dissipation. The y^+ value is a measurement of distance from the wall with relation to the laminar layer calculated using the friction velocity of the layer. The guideline states that a y^+ value of 30 is a good goal. Considering the high Reynold's number of atmospheric flows, higher values of y^+ up to 50 or 100 are acceptable.

The y^+ value is calculated by:

$$y^+ = \frac{u_*^* y}{\nu} \quad (4.1)$$

where y is the distance to the center of the first cell from the surface, u_* is the friction velocity, and ν is the kinematic viscosity of air.

D. Guidelines on grid design - Guideline 11.8:

For hexahedral cells, gridlines should be optimized in an effort to achieve $\sim 90^\circ$ for all sides. Included angles of less than 40 or more than 140 degrees deteriorate the results. Avoid non-orthogonal cells near boundaries (surfaces and domain boundaries). Avoid aspect ratios that are too high (ratio of one edge of the cell to the perpendicular edge). The goal should be to maintain an aspect ratio of near 1:1 in areas of importance in the domain, but no greater than 5:1 (CFD2000, 2002). The ERCOFTAC guidelines state that ratios as high as 20 - 100 can be satisfactory, and we have found this acceptable for regions near the outer edge of the domain. Expansion ratios of cells (the increase in cell length from one layer of cells to the next) should also be kept at a minimum, following recommendations by the code creator (1.3 is the maximum expansion ratio recommended for CFD2000).

E. Guidelines on temporal discretization - Guideline 11.10.4:

Second order accuracy is recommended in both space and time. Also conduct sensitivity analyses by varying the time step, changing grid size, and by trying higher order schemes for convection.

4.2.2 Guidelines from the COST Action C14 Working Group 2

COST (European COoperation in the field of Scientific and Technical research) is a framework for the cooperation of research institutions in Europe on a matter of pressing subjects. Action C14 is the study of the “Impact of Wind and Storms on City Life and the Built Environment,” and is part of the Urban Civil Engineering group of COST. Working Group 2 of Action C14 is dedicated to CFD techniques involving the analysis of urban wind climate. The main focus of the group is pedestrian climate, but its efforts can be applied to other urban applications such as air quality modeling. Their set of guidelines is also based off of recommendations from the QNET-CFD and ERCOFTAC guidelines.

The following list includes some of the more important guidelines from their publications available at <http://www.costc14.bham.ac.uk>. (Franke, 2004):

- Use of the RNG model is suggested over K- ϵ or K- ϵ variants, in order to use an anisotropic turbulence model
- Area of radius for a project: ~ 300 m around a region of interest
- Buildings within 6-10 times their own height distance from a project should be included in the model
- Geometrical details with size > 1 m should be included in the model in the region of most interest
- Surrounding buildings should be simple blocks with less detail
- The domain sides should be $5H$ in distance upwind and laterally
- Domain top should be $6H$ above ground
- Domain outlet downwind should be $15H$ in distance from the last structure
- Blockage ratio of buildings for incoming wind should be $\leq 3\%$
- Lateral and top boundaries should include symmetry and no re-entry of the flow
- The domain outlet should have a zero gradient for all variables
- Use of the Richards and Hoxey (1993) equations for wind, TKE, and ϵ profiles
- Smooth walls for pedestrian comfort study with a higher density of cells nearer the surface
- For pedestrian comfort, the height region of interest for pedestrian wind speed should be at the 3rd or 4th cell from the surface
- Use second order methods for advection and diffusion for a final solution
- Demonstrate grid independent solutions: refine model by 50% more nodes in each direction.

4.2.3 QNET-CFD

QNET-CFD is the “Thematic Network on Quality and Trust for the industrial applications of Computational Fluid Dynamics.” It is a European program formed to provide industry with guidance on CFD techniques and quality control for industrial applications. QNET-CFD guidance is divided into 6 thematic areas. Two of these areas of focus, “Environmental Flows” and “Construction and HVAC”, involve micro-scale air quality evaluation problems. Because of this direct focus on selected applications, QNET-CFD is a good reference for guidelines on any CFD project (QNET, 2005).

The guidelines for each thematic area were developed by different teams performing baseline type projects and recommending engineering advice based on their research and experience with these baseline projects. Each baseline project involved a physical test where data was gathered on physical properties of the flow. The QNET project involved simulating each physical study using CFD and comparing the results.

There are some differences in the guidelines for each application. A user should be able to judge by reviewing the baseline project if the provided guidance is applicable to his/her study. The following sub-sections contain specific guidelines for both related Thematic Areas.

4.2.3.1 Thematic Area 4: Best Practice Advice for Civil Construction and HVAC

Although this section covers both hydraulics and transport infrastructure, the main portion of it focuses on the built environment for both external and internal flow. Five applications were demonstrated for this thematic area, each concluded with best practice advice. For micrometeorological air quality studies, only one of these projects was directly similar - “Wind Environment Around an Airport Terminal Building” (Scaperdas and Gilham, 2004).

The following best practice advice is recommended in the discussion of this project:

- A 3-D calculation should always be used.
- The computational domain should be no smaller than 5H upstream, 15H downstream, and 4H on either side.
- Simplification of building geometry is necessary and a refinement of all details down to 0.01H is recommended if the details may have influence on the region of interest.
- A gradual expansion ratio of 1.2 can be applied.
- The inlet boundary conditions should use the wind, TKE, and ϵ profiles recommended by Richards and Hoxey (1993), and Castro and Apsley (1997). Both sets of profile equations have logarithmic wind profiles. Castro and Apsley’s conditions contain a distinction for TKE based on a

surface layer (up to $0.9H$) and above the surface layer. The ϵ profiles are similar.

- The ground boundary should be applied with a rough wall with appropriate z_0 value.
- Unsteady RANS equations give better results. LES is the best option.

4.2.3.2 Thematic Area 5: Best Practice Advice for Environmental Flows

For this thematic area, five applications were demonstrated for practice advice, four of which directly relate to urban microenvironment applications. Each application and the best practice advice for each are discussed below:

1. Flow and Dispersion in the Presence of an L-shaped Building:

This application concerns the experience of a firm with the EMU project described earlier in this paper. This project concerned the dispersion of a non-buoyant tracer gas around an L-shaped building. The best practice advice for this type of application is:

- Computational domain with sides at: $8H$ upstream, $15H$ downstream, and $6H$ vertical
- $0.2H$ horizontal grid spacing in the region of the source and building.
- $0.05H$ vertical grid spacing in the region of the source and building
- Expansion ratio of no more than 1.2
- Maximum horizontal grid resolution of $2H$
- Maximum vertical grid resolution of $0.5H$
- 2nd order accurate numerical schemes, under-relaxation factors avoided
- Advanced RANS or LES

2. Dense Gas Release over flat terrain with and without obstructions:

This project involved the continuous jet release of a cold dense gas over flat ground. Dispersion over the flat surface and around an obstacle on the surface was simulated. The best practice advice for this project was as follows:

- Vertical velocity at the top of the domain should be kept at zero.
- Ground heat transfer should be limited to conduction.
- Size of the domain should be at least $8H$ upstream, $15H$ downstream, and $6H$ vertically.
- Expansion ratio of 1.2
- Underground domain should be a depth of $1H$ with 10 cells vertically.

3. Urban Scale Problems:

This effort involved modeling the dispersion of exhaust in a 2D array of buildings with emphasis on the concentrations in the canyons between the buildings.

- 2-D idealization is suitable for street canyon modeling when the wind is perpendicular to the street axis.

- An asymptotic roughness and displacement height is needed to reflect the urban nature of the domain.
 - Domain including 2 canyons upstream and two downstream is adequate.
 - A horizontal resolution $< H/10$ has little further effect on accuracy (i.e., $0.1H$ resolution is good enough to accurately model the flow).
 - A vertical resolution of $H/10$ is adequate.
4. Flow and Dispersion over isolated hills and valleys:
This project involved modeling the dispersion of pollutants from a stack located in the wake of a hill. The physical test was conducted in the EPA wind tunnel. The Best Practice Advice for this project is as follows:
- Upper boundary should be $10H$ above the hill.
 - Surface should be fully rough.
 - Downstream outlet should be at $20H$ behind hill (depends on area of interest for exposure to pollutant).
 - 2nd-order differencing for convective terms is crucial.
 - Horizontal mesh of $0.1H$ at hill summit is best.
 - Vertical mesh of $0.01H$ at hill summit is best.
 - Proper wind and turbulence profiles are necessary.
 - Avoid using the standard $K-\epsilon$ model - more advanced model needed.
 - Unsteady flow should be used.

The environmental flow thematic area discussion is wrapped up with a discussion on best practice advice that is common for all projects of this type. Some of these points are as follows:

- Coriolis force can be ignored for small-scale surface layer flow modeling.
- Modeling of buoyant forces is necessary for realism.
- Larger scale modeling will make the incompressible assumption invalid.
- 2nd-order accuracy is necessary.
- LES is recommended over RANS modeling.
- 3-D pollutant dispersion modeling requires non-isotropic turbulence parameters to account for the differences in directional dispersion.

4.2.4 Project EMU Conclusions - Best Practice Advice

Based on the results of Project EMU, which is described in more detail in section 5 of this chapter, the authors were able to provide a set of best practice advice. However, they are rather vague compared to the other guideline sets. They note that as the scenarios became larger and more complex, it was increasingly more difficult for the teams to satisfy common best practice advice. Due to this, problem size limits the applicability of best practices. The list of recommended guidelines is summarized as follows:

- Objectives: The user should have a clear pre-modeling plan with emphasis on how uncertainty is to be handled. The plan should include detail on

how the domain setup will fit to the test with more detail in regions of interest.

- Preliminary “scoping” calculations: Domain size and modeling time should be estimated to give a proper estimate of cost and time to the client.
- Domain size: Follow the common 5H rules for domain side distance from obstacles and be careful to have a long enough domain to account for pollutant transport.
- Mesh Architecture: Finer mesh is needed near sources and around buildings. The author points out that mesh independent solutions are “generally not achievable with this class of problem.”
- Boundary conditions: Realistic atmospheric boundary layer profiles of wind and turbulence are needed.
- Numerics: Use of higher-order differencing (2nd order or greater).
- Turbulence model: standard K-ε model is adequate near the building, but a model tuned for atmospheric flows would be better for far-field dispersion.
- Time accuracy: It is important to pay attention to the Courant number. This is a limit on the time step of the calculation and is defined by:

$$C = \frac{\Delta t}{\Delta x_{cell} / u_{fluid}} \quad (4.2)$$

- Quality assurance: QA plan should be prepared before the project and followed closely.
- Output: Careful planning before project to ensure that analysis methods are correct.
- Resources: CFD user experience with software, code, and dispersion science is crucial. They found 4 to 6 months of experience with the CFD code was necessary to achieve reasonable results.

5 Validation and Verification

Computational modeling of any type is absolutely worthless without a rigorous effort to validate the approach to the physical phenomena it is meant to simulate. This is a critical issue in CFD today when we consider that CFD itself is extremely complex and that the physical processes being modeled (turbulence, heat transfer, diffusion, etc.) are not entirely understood or resolved mathematically. Thus, an ongoing effort of model improvement through verification is necessary before any claim can be made about the predictability of a model.

CFD, under its various forms, has been validated for many different types of flow phenomena. For computational wind engineering and micro-scale urban dispersion, this has been somewhat of a challenge. Verification studies have

demonstrated a number of difficulties in micro-scale meteorological modeling using CFD in its various forms, but also significant and useful results.

The main difficulty has been in the complexity of bluff body flows. Flow around a fixed object is inherently transitory and characterized by vortex shedding. This fact considerably impairs the credibility of steady state modeling. It has been observed that “separation and re-circulation regions develop, wash away resulting in uniformly down-wind flows over the roof, and then the circulation zone redevelops” (Meroney, 1999). Also, bluff body flows can contain separation zones and re-circulation zones that can not be accounted for well in the standard log-law wall functions.

The isotropic turbulence assumption is problematic in the surface layer of the atmosphere. In the atmosphere, the size and scale of turbulent eddies is dictated by the presence of the ground and the static stability of the atmosphere. Thus, eddies have an easier time moving laterally than vertically. Pollutant dispersion is mainly determined through turbulent diffusion, so directional spread of the turbulent eddies is very important.

5.1 Flow Around a Block

Much of the validation work of CFD for wind engineering involves studying the simulated flow around a simple cube. This is a great validation exercise for buildings because most buildings consist of groups of cubes and rectangles. Even though the geometry is simple, the flow around a simple block is quite complex involving strong pressure gradients, streamline curvature, separation and reattachment, and re-circulation zones (Scanlon, 1997). Also, a great deal of wind-tunnel data is available to ensure that the details of the flow around a block are well described, such as that by Castro and Robins (1977), which is a common study referred to for CFD validation.

Murakami and Mochida (1989) were among the first to conduct validation studies of CFD modeled flow around a block. They carried out a series of CFD runs and compared them to wind-tunnel studies of flow around a 200 m cube. Their studies demonstrated that meshing of around $0.17H$ produced poor results in velocity direction and magnitude around all parts of the block. Best results were produced when mesh resolution was increased to about $0.04H$ around the entire block, including the lee of the block where re-circulation zones were sensitive to the mesh interval. They demonstrated that with sufficient mesh resolution the flow around the block and surface pressure distributions, including recirculation zone position and magnitude, was simulated rather well.

As previously described, Murakami and Mochida also found that the $K-\epsilon$ model had difficulties in accurately predicting TKE and ϵ . First, they found that the mesh in the lee of the block had to be fine enough to accurately promote the production of TKE and ϵ . Under-prediction of TKE tends to elongate the size of the re-circulation zone. They also noted the common over-production of TKE at

the windward sharp edge of the block, and attributed it to the inability of the wall function to handle separation at this point.

K- ϵ variant models such as the MMK model, discussed earlier, were found to improve model performance at the sharp edge, but it did not improve flow in the wake, as it tended to over-predict the lengths of the recirculation zones. The Chen-Kim and RNG models showed more success at improving the predictability of the flow around a building.

The findings of Murakami and Mochida suggest that the K- ϵ model is good at predicting flows around a block, but needs improvement if dispersion around the block is going to come into play, considering that accurate representation of TKE is needed to model the dispersion correctly. Many studies have been conducted that involve the dispersion of exhaust around a cube. Generally, they have found that in neutral flow conditions the K- ϵ model reasonably predicts ground concentrations of pollutants released at the roof level (Zhang, 1996 and Scanlon, 1997). Concentrations tend to be overestimated on average, which is good for a conservative air quality evaluation.

5.2 Dispersion in a Street Canyon

The case of dispersion of pollutants in a street canyon, both with the source inside and outside of the canyon, has been a significant focus of air quality study. It is important because of the high concentrations of carbon monoxide and diesel particulate matter in dense urban topography that consists primarily of street canyon grids. In these arrangements, “skipping flow” often occurs, trapping the pollutants in the canyon. Because of these concerns and the relatively simple geometry of the case, it is a useful baseline case for CFD validation studies.

Most validation studies involve analyzing the positioning of streamlines within the canyon and the magnitude of velocity at certain points within the canyon. Also, TKE within, above, and at the walls of the canyon can be compared to experiments. Since the dimensions of street canyons can vary in width and building wall heights, a lot of attention has been directed to the difference in flow and dispersion with varying dimensions. The common aspect ratio, which is the ratio of canyon width to building wall height (the baseline case always considers canyon wall buildings to be the same height), is often the focus of attention in studies.

Baik and Kim (1999) conducted a numerical study of flow and dispersion in street canyons with different aspect ratios using the “Realizable” K- ϵ variant model. The study focused more on the nature of the flows rather than comparison to experimental results. However, their results did indicate that the vertical velocities at the canyon walls in a canyon with aspect ratio Height/Width = 1.2 was close in magnitude to that of a wind-tunnel study. They also say the locations of TKE maxima and minima are the same as found in experimental studies.

Sagrado et al. (2002) conducted a numerical study of pollutant dispersion in a street canyon as a validation, with their results directly compared to experiment. The numerical simulations were conducted using the “Realizable” K- ϵ variant model. This study was conducted using blocks separated by an aspect ratio of 1, with both canyon walls the same height for the first case and the lee canyon wall higher in the second case. The study also took into account a case where an upstream building influenced flow at the canyon. The results of the numerical simulation are qualitatively quite similar to that of the experiment; the streamlines, re-circulations, and separation points are almost identical in most cases. However, the velocity magnitudes and pollutant concentrations differ quantitatively. The authors indicate that the discrepancies may be due to the weaknesses of the 2-D steady state solution, suggesting it cannot account for the 3-D, unsteady characteristics of real flow.

5.3 Dispersion Over a Flat Field

Another baseline validation study is the dispersion of a tracer in the atmosphere over a flat field. This is an important validation effort because it tests the model’s scheme to disperse pollutants within the atmospheric boundary layer. As discussed earlier, models with isotropic turbulence assumptions cannot account for the directional differences in turbulent flux in the surface layer.

Most validation studies have involved comparing numerical CFD results to measurements from the famous “Project Prairie Grass,” consisting of 70 scenarios of neutrally buoyant gas releases over an open agricultural field. This and several other studies were combined to determine the standard Gaussian vertical and horizontal dispersion coefficients that are still used in many of today’s air quality models, such as EPA’s SCREEN and ISCST3.

Tang et al. (2005) have been active in validating RANS modeling for dispersion over a flat field by comparing their numerical results to the “Project Prairie Grass” results. Their work involves not only comparisons at plume centerline, which is common of many studies, but also of measurements away from the centerline, along an arc. Since they use the standard K- ϵ model in their study, they accounted for anisotropic turbulence in the atmosphere by modeling a spread of wind direction to include the variance in wind direction for a standard average wind. In the study, the centerline and arc concentrations compare very well to the experiment when Schmidt numbers of around 1.0 are used.

5.4 Project EMU

Project “Evaluation of Modelling Uncertainty” (EMU) (Hall, 1996) is likely the most well known “CFD as a micro-scale air quality model” validation exercise. The Project was conducted for the European Commission’s Science, Research, and Development section to explore the usefulness of CFD as a tool to model

atmospheric dispersion around buildings. The goal of the project was to investigate the variance in results from different modelers given the same CFD problem and the accuracy of those results when compared to experimental measurements. The same cases were modeled in a wind-tunnel and the results compared to each CFD run.

This project has been referred to as an indication of the significant variability that can occur due to user choices concerning gridding, boundary conditions, numerical scheme, and other variables. In this project, four separate teams were given the details of a project and were asked to conduct CFD modeling using the same commercial CFD code. The project involved three different stages, increasing in complexity:

- Stage A: Dispersion of a gas around an L-shaped building under a neutrally stable atmosphere at 5m/s wind speed. Gas was released in several different scenarios: a continuous release of neutrally buoyant gas, a semi-continuous buoyant jet, and an instantaneous release of dense gas.
- Stage B: A second building, a cliff, and a trench were added to the domain with a stably stratified atmosphere at 2 m/s. A denser gas was used in several different release scenarios.
- Stage C: Full industrial site with many buildings and complex terrain. Dense gas released under different scenarios in a neutral atmosphere.

The teams were only given the dimensions, gas release scenarios, and atmospheric conditions. The goal of the project was to examine how each team set up their domains, meshing, atmosphere, and boundary conditions, and to see how the results varied based on their decisions. Overall, there was substantial difference in all factors. Meshing, boundary condition setup, and numerical differencing were found to have a lot of influence on the accuracy of the solutions. In the literature, emphasis has been placed on reviewing the results of Stage A because if the simple case is problematic, then the results from a more complex case will be even more suspect.

In general, for Stage A, two of the teams conducted their modeling more in line with the common best practice advice discussed in the next section of this paper and had better results compared to the teams that deviated from it. Teams #1 and #2 used second-order differencing terms as well as a denser mesh nearer the buildings, with Team #2 using the densest mesh. Team #3 used a small domain, only extending 2H upwind, whereas the other teams have domains that extended to 5H or greater upwind, as indicated in common best practice advice. Teams #3 and #4 used a smooth ground, which leads to elongated plumes along the surface. Teams #1 and #2 used more realistic atmospheric boundary layer profiles of turbulence (#1 used a wind tunnel profile, #2 used the Richards and Hoxey [1993] equations).

For results for a neutrally buoyant plume, Team #2 performed very well with estimated concentrations at different points downwind of the building very near to

the wind tunnel measurements. Team #1 had poorer concentration results, but the plume dimensions (5% iso-concentration field) were close to experimental results. Teams #1, #3, and #4 deviated from the experimental results substantially.

For Stage A with a buoyant jet, Team #1 accidentally applied a neutrally-buoyant jet, so the results are not comparable. Teams #2 and #4 had fairly similar plumes and #3 had a shorter, less spread plume. Plume dimensions are fairly close to the experimental results for Teams #2, #3, and #4, with Team #3 predicting the downwind hazard length a bit better due to less plume spread.

For Stage A with a dense cloud release, Team #1 again specified a neutrally buoyant gas so that the plume blew over the building roof instead of sagging around the building as observed by the other teams. Team #3 deviated a bit with their cloud not sinking around the building as much as #2 and #4. Teams #2 and #4 have fairly similar results. This case was not modeled in the wind tunnel so a comparison could not be made.

Overall, Project EMU demonstrated the high potential for inaccuracy of CFD results due to the many degrees of freedom a user has in selecting parameters that affect the quality of the solution. Human error, such as in the selection of ground roughness, the selection of a neutrally buoyant gas instead of a buoyant gas, or the wrong direction of heat flux at the surface, proved to be the greatest cause of errors. In addition, a number of mistakes were made in concentration calculations in post-processing. Domain size and cell size variance had a large influence on the accuracy of the results, generally with higher resolution and following the 5H domain rule leading to more accurate results. Turbulence profiles in the atmospheric simulation had influence on the results, with some of the teams applying unrealistic conditions. The teams using realistic turbulence profiles tended to have more accurate results.

Some important overall conclusions were made based on the project results. An important detail discovered from this effort was that the CFD solution most free from numerical error was not necessarily the most accurate CFD solution. Hazard ranges were often over-predicted. The results of the stable atmospheric cases were quite poor with substantial spread in the teams' results.

The Project EMU conclusions illustrate the degree of caution that must be used when reviewing atmospheric urban environment CFD results. However, the degree of variability found in this study is not inevitable. When user error is limited by active quality control and the guidelines provided here are followed, then much of the variability found in the Project EMU study can be avoided. One could conclude from the study that gas dispersion in a neutral atmosphere can be done accurately with CFD if the proper approach is followed.

5.5 Validation Exercise Recommendations

Before conducting a CFD study, it is important to validate and verify the user/code combination. One should first conduct several validation studies using baseline scenarios. The document “How to verify, validate, and report indoor environment modeling CFD analyses” (Chen, 2001) is a good document for reference. It discusses the importance of validation before attempting to use CFD for a specific project, with an emphasis on indoor problems. The document also suggests several studies with adequate data that can be used for indoor validation work. Since no similar document exists for external flow at the scale we are concerned about in this chapter, we suggest that the four types of studies explored above be used as a first step verification/validation:

- Flow around a block: Possibly use data from Minson (1995), Snyder (1994), or Castro and Robbins (1977)
- Flow within a street canyon
- Flow over a flat field: Horizontal and Vertical dispersion coefficients are available in Turner (1970)
- Project EMU, Case A1 and A2: Good measurement details for flow and dispersion around a simple building (Hall, 1996)

5.6 Example Validation Exercise

This is an example of a quick qualitative validation exercise. Snyder and Lawson (1994) conducted a wind-tunnel study of the flow around a simple cube in the EPA wind tunnel. Wind vectors were measured at certain points along the center of the domain and streamlines were estimated by a plotting algorithm. The results of this study include generally good estimates of streamlines, separation points, and reattachment lengths. However, some of the length estimates of the block wakes are not especially accurate because of the sparse velocity measurements downwind of the block.

Our intention in this validation exercise is to simulate the wind tunnel experiment using the wind and turbulence equations, and setup procedures discussed in section 3 of this chapter. Boundary conditions and settings will be set up appropriately to follow the guidance and methods described in this paper, ensuring that the domain, wind and turbulence profiles, and other parameters match the experiment as closely as possible.

We begin our validation exercise by constructing the domain. The cube itself was the standard 200 mm surface mounted cube that is generally used in bluff body flow validation (Castro and Robbins, 1970). A description of the EPA wind tunnel is available in Snyder (1979). For a CFD domain we apply a space of 8H upstream, 15H downstream, and 6H laterally to the domain walls. This domain has larger dimensions than recommended to provide extra room to examine the boundary layer. The top of the domain was 9H above the top of the cube to provide a 2 meter high boundary layer to coincide with the wind tunnel

dimensions. The outlet boundary was a standard pressure outlet that has no effect on the upstream flow. The sides and top of the domain are frictionless walls. The inlet is set at the upstream boundary with incoming wind and turbulence profiles nearly identical to those of Snyder and Lawson (1994). The wind and turbulence profiles and domain setup are illustrated in Figure 7.

It is important to ensure that the wind profile and turbulence profiles match the experiment as closely as possible. It has been demonstrated that upstream turbulence has significant effect on the size and positions of flow characteristics around a building. Higher turbulent energy in the flow will result in a reduced building re-circulation cavity (Zhang, 1992).

Snyder and Lawson include in their paper a plot of wind velocity measured at four different points along the stream in the wind-tunnel before the block was placed in the stream (two upstream of the block position and two downstream of the block).

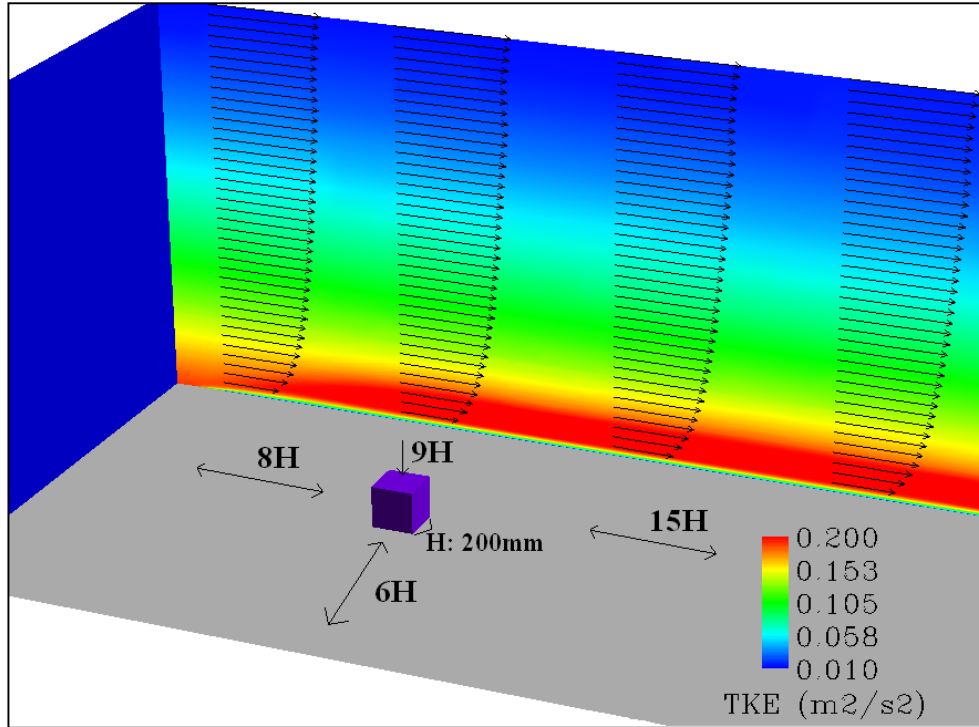


Figure 7. Illustration of the CFD domain setup for the sample qualitative validation study. Domain boundary distances from the 200 mm cube are indicated. Wind profiles at various points along the domain are illustrated. Turbulent Kinetic Energy values are illustrated in scalar coloring.

The plot demonstrates that the wind profile is quite continuous across the domain with very little deviation. They indicate that the profile is consistent with a 0.16 coefficient power law profile. However, by our examination of the data, a power law coefficient of 0.176 seems to fit with the data better. The power law equation is often used to describe a wind profile instead of the log law equation. The common power law equation is:

$$\frac{U(z)}{U_{z_0}} = \left(\frac{z}{z_0} \right)^n \quad (5.1)$$

where U_{z_0} is the windspeed at a reference height z_0 and n is the coefficient. Typical values of n for different types of terrain can be found on Figure 10.5 of Arya (1988).

Snyder and Lawson compare the turbulence intensity profile to the bounds suggested by the Engineering Sciences Data Unit (ESDU) for turbulence in a neutral atmosphere with full-scale roughness lengths between 5 and 50 cm. The wind-tunnel is set up to simulate a full scale friction element length of 20 cm (actual roughness length in the wind-tunnel was 1mm), so it is assumed that the turbulence profile will fit within this range.

Turbulence intensity is a bit more variable along the domain at the center of the domain, about H to 4H above the surface (0.2 to 0.8 m). Turbulence intensity diminishes in this region along the domain so that the incoming intensity is greater than the ESDU bounds and the outgoing intensity is less than the ESDU bounds. The average of the intensities fit well within the ESDU bounds, and the intensities nearer to the block position are near the average.

For the CFD domain profile equations we use the Richard and Hoxey equations (3.2, 3.7, 3.8, and 3.9 in this chapter). We begin by calculating the profiles using these equations and compare them to the Snyder and Lawson profiles to ensure that they are the same. The first step is to calculate friction velocity using Equation 3.2 in this chapter since the profile equations are based on it. The friction velocity should be constant throughout the layer for a neutral boundary layer. Twelve different elevations are selected for measurement and we calculate friction velocity at each level using the velocity and height at each level with the roughness element height of $z_o = 0.001$ m. The values are given in Table 6 using a von Karmon constant κ of 0.42. The experimental measurements used for our calculations may not be exact; they were picked off the graph in Figure 1 of Snyder and Lawson (1994).

Table 6. Wind Profile Setup Calculations.

Height (m)	Wind speed measured (m/s)	Friction Velocity (m/s) from Eq. 3.2	Calculated from Eq. 3.7 using 0.24m/s u_*	Wind speed: power law Eq. 5.1
0.05	2.3	0.246	2.25	2.30
0.1	2.7	0.246	2.64	2.60
0.2	3.1	0.246	3.03	2.94
0.4	3.4	0.238	3.43	3.32
0.6	3.7	0.243	3.66	3.56
0.8	3.8	0.239	3.82	3.75
1.0	3.9	0.237	3.95	3.90
1.2	4.0	0.237	4.05	4.02
1.4	4.1	0.238	4.14	4.13
1.6	4.2	0.239	4.22	4.23
1.8	4.3	0.241	4.28	4.32
2.0	4.4	0.243	4.34	4.40

The friction velocity for the layer averages about 0.24 m/s, which corresponds to u_*/U_R (U_R is the velocity at the top of the boundary layer) of about 0.05, which was the value calculated by Snyder and Lawson. Using this friction velocity, we can now calculate the wind profile and compare it to the experimental data. The calculated winds, included in Table 6, fit well to the experimental winds, justifying the use of the log-law wind Equation 3.7. The results are also compared to a power law wind equation using an exponent of 0.176 in Table 6.

Comparing turbulence intensities is a bit more difficult since turbulence intensity and turbulent kinetic energy are not exactly related. Turbulent kinetic energy can be estimated from turbulence intensity. Turbulent intensity is (u'/\bar{u}) , so mean turbulent kinetic energy can be estimated from the magnitude of u' . The kinetic energy equation can be used to estimate turbulent kinetic energy per unit mass:

$$TKE = \frac{3u'^2}{2} \quad (5.2)$$

The estimated TKE from this equation is included in Table 7. Observing the resultant TKE profile, we see that TKE decreases with height. This means we cannot use the Richards and Hoxey equation for TKE (Equation 3.8), which is based on the assumption of constant TKE in the surface layer. Their assumption is often only valid when the boundary layer is deep and the roughness elements are small. Therefore, the alternative TKE and ϵ equation (Equations 3.3 and 3.5) from Huser et al. (1997) are used. The TKE curve with a C_μ of 0.024 fits the TKE profile best using Equation 3.3. TKE calculated from the equation fits well to the ESDU bounds and wind-tunnel TKE profiles.

Table 7. TKE Profile Setup Calculations.

Height (m)	Turbulent Intensity (measured)	Wind Speed measured (m/s)	Estimated TKE (m^2/s^2) Eq. 5.2	TKE Eq. 3.3 (m^2/s^2) Using $\delta=3.4$ m and $C_\mu = 0.024$
0.05	0.22	2.3	0.384	0.361
0.1	0.18	2.7	0.354	0.350
0.2	0.15	3.1	0.324	0.329
0.4	0.13	3.4	0.293	0.289
0.6	0.11	3.7	0.248	0.252
0.8	0.10	3.8	0.217	0.217
1.0	0.09	3.9	0.185	0.185
1.2	0.08	4.0	0.154	0.156
1.4	0.07	4.1	0.124	0.129

The first test runs reveal that the TKE profile does not maintain itself throughout the domain, fading slightly from inlet to outlet. Therefore, a constant source boundary condition is applied to the domain to supply TKE at a specified rate to balance the excess dissipation. Tests demonstrated that a source equal to amount 70% of the dissipation rate in TKE production would maintain a constant profile throughout the domain. A source above 70% produced an exiting profile with higher TKE values than the entering profile, while a source below 70% of the dissipation rate did not compensate fully for the excess dissipation.

Simple mesh sensitivity runs were conducted beginning with a mesh of 0.0625H at the cube with expansion ratios of up to 1.4 near to the cube. This original mesh was used to account for the y^+ value near the ground. Expanding to a mesh of 0.125H dramatically reduced the predictive quality of the flow around the block and seemed to alter the nature of the turbulence profile. Concentrating the mesh down to 0.03H did not significantly improve the results; the flow around the block did contain more evident re-circulation on the roof, but other details such as the consistency of the TKE profile did not improve significantly.

All final runs were conducted using the Chen-Kim K- ϵ model with second-order terms, and the PISO differential equation solver in CFD2000 by Adaptive Research. Local time-stepping was used to accelerate convergence. Steady state was usually reached around 30 - 40 seconds for most cases, and all runs were run out to 60 seconds. The constants of the Chen-Kim K- ϵ model were set at $C_\mu = 0.024$ and $\sigma_\epsilon = 2.37$, with the others set to their defaults.

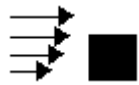
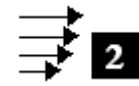
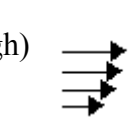
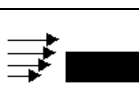
The results of the modeling runs were compared to the results of Snyder and Lawson (1994). Ten different runs were conducted with the incoming wind perpendicular to the windward face of the cube. Each run involved different block dimensions varying in three different orientations: varying in length parallel to the wind flow, varying in length normal to wind flow, and varying in height.

For each case, the separation point at the windward side of the block and the length of the re-circulation zone behind the block were estimated and compared to those of Snyder. The results are provided in Table 8. It compares the results of our CFD runs and the Snyder and Lawson wind-tunnel results to a commonly used set of empirical equations based on observations from Hosker (1984). Hosker developed the equations from earlier wind-tunnel studies of flow around different sized blocks. The equations are used to estimate the length of the wake behind the block.

The first equation is used for block buildings where $L/H \leq 2$:

$$\frac{X_r}{H} = \frac{L}{H} + \frac{A(W/H)}{1+B(W/H)} \quad (5.3)$$

Table 8. Results of the Sample CFD Validation Exercise.

Scenario	Snyder Wake length/ Height	Hosker Wake length/ Height	CFD validation example Wake length/Height
Cube 	1.4	1.5	1.7
2W 	2.1	2.6	2.5
4W 	3.5	4.2	3.5
10W 	5.6	6.7	5.5
Plate (1H high) 	2.3	not applicable	2.5
½ L 	1.5	2.2	1.5
2L 	1.2	1.4	1.5
4L 	1.4	1.4	1.5
2H 	0.75	1.2	1.4
3H 	0.5	1.0	0.8

where X_r is the wake length, L is the building along-wind length, W is the width, H is the height and A and B are scaling functions of L and H :

$$A = -2.0 + 3.7(L/H)^{-1/3} \quad (5.4)$$

$$B = -0.15 + 0.305(L/H)^{-1/3} \quad (5.5)$$

Hosker compared this curve to other studies and found that most data is within $\pm 15\%$ of the equation estimate.

For buildings where $L/H \geq 2$, the equation is:

$$\frac{X_r}{H} = \frac{1.75(W/H)}{1 + 0.25(W/H)} \quad (5.6)$$

All of the CFD results showed fair agreement with the wake lengths and very good agreement for separation points on the windward wall. Overproduction of TKE at the sharp windward edge was evident in every run, likely leading to error in flow magnitudes downwind. The recirculation zone on the top of the block is minimized in some of the cases. Qualitative comparison of the streamlines showed some deviation when compared to the Snyder and Lawson results, though the center of circulation was often in approximately the same location. A graphical comparison of the base case (the simple cube) is shown in Figure 8.

This example has been a demonstration of the simplest form of validation exercise. A more exhaustive set of validation exercises must be conducted to confirm the user-code combination before conducting an actual project. As well as qualitative comparison of streamlines, the validation exercise should involve comparison of separation and re-attachment lengths and centers of circulation. Quantitative comparisons of surface pressures, TKE, and velocity are also recommended. A good set of validation exercises are suggested in section 5.5.

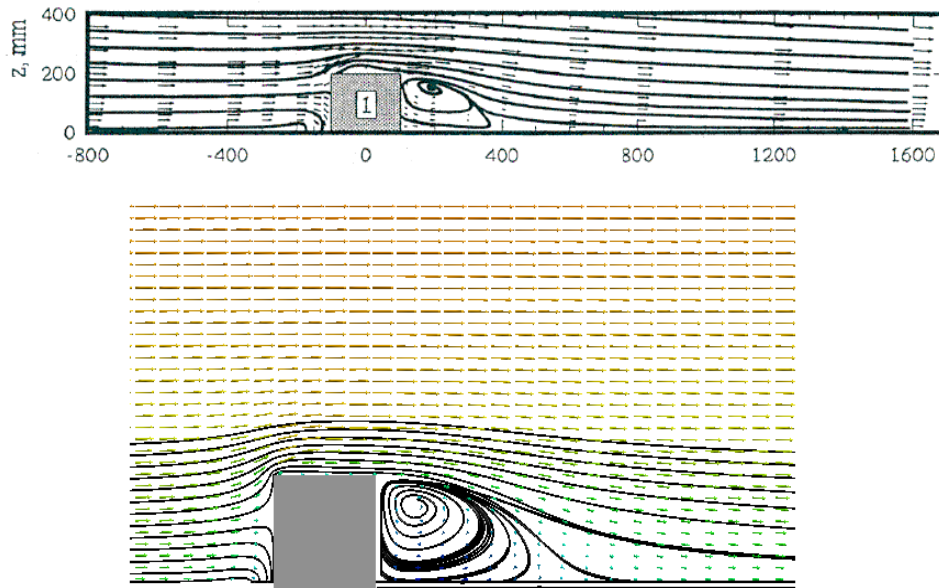


Figure 8. Graphical comparison of the streamlines around the simple cube. The top graphic is the results of Snyder and Lawson (1994). The bottom graphic is the illustration of the simple validation exercise results using CFD.

6 Conclusion

In this chapter we have discussed applying CFD to local-scale urban air quality dispersion studies. The purpose of this document is to supply the typical environmental scientist or engineer with an overview of the methods and details of CFD modeling for urban micro-environments.

The methods and guidelines that have been presented are best used for simpler small air quality studies around a single building or several buildings. We have reviewed the general methods of setting up and conducting a study using the K- ϵ model and its variants. This involves setting up proper boundary conditions to simulate the atmosphere, proper meshing and mesh sensitivity tests to ensure grid independent solutions, selection of wind scenarios, and visualization techniques.

The discussions presented in this chapter can be utilized as best practice guidance based on the most recent computational wind engineering studies using simpler K- ϵ methods.

References

Adaptive Research. 1997. *CFD2000 - Theoretical background*. Adaptive Research, Division of Simunet Corporation, Alhambra, CA.

- Adaptive Research. 2002. *STORM/CFD2000 User Guide*. Adaptive Research, Division of Simunet Corporation, Alhambra, CA.
- Apsley, D., 2003. Lecture notes for Introduction to CFD, Spring 2003. University of Manchester, School of Mechanical, Aerospace and Civil Engineering.
- Arya, P., 1988. *Introduction to Micrometeorology*, 1st edition. Vol. 42 of Int. Geophysics Series. Academic Press, New York.
- Baik, J. and J. Kim, 1999. A Numerical Study of Flow and Pollutant Dispersion Characteristics in Urban Street Canyons. *Journal of Applied Meteorology*, Vol. 38, pp. 1576-1589.
- Baik, J., J. Kim, and H. Fernando, 2003. A CFD Model for Simulating Urban Flow and Dispersion. *Journal of Applied Meteorology*, Vol. 42, pp. 1636-1648.
- Bartis, J., D. Vlachogiannis, and A. Sfetsos, 2004. Thematic Area 5: Best Practice Advice for Environmental Flows. *QNET-CFD Network Newsletter*, Vol. 2, No. 4, July 2004.
- Bottema, M., 1997. Turbulence closure model “constants” and the problems of “inactive” atmospheric turbulence. *Journal of Wind Eng. and Ind. Aerodynamics*, Vol. 67 & 68, pp. 897-908.
- Brown, R., 1991. *Fluid Mechanics of the Atmosphere*. Vol. 47 of Int. Geophysics Series, Academic Press, San Diego.
- Castro, I. and A. Robins, 1977. The flow around a surface-mounted cube in uniform and turbulent streams. *Journal of Fluid Mechanics*, vol. 79, part 2, pp. 307-335.
- Castro, I. and D. Apsley, 1997. Flow and dispersion over topography: a comparison between numerical and laboratory data for two dimensional flows. *Atmospheric Environment*, Vol. 31, No. 6, pp. 839-850.
- Castro, I., 2003. CFD for External Aerodynamics in the Built Environment. *QNET-CFD Network Newsletter*, Vol. 2, No. 2 – July 2003.
- Chen, Y. and S. Kim, 1987. Computation of Turbulent Flows Using an Extended K- ϵ Turbulence Closure Model. *NASA Contractor Report 179204*.
- Coirier, W., 2004. Validation of CFD-Urban using Accepted Open Field and Urban Area Transport and Dispersion Test Data. *8th Annual George Mason U. Conf. on Transport and Dispersion Modeling*. July 14, 2004, Fairfax, Virginia.
- Delaunay, D., 1996. Numerical simulation of atmospheric dispersion in an urban site: Comparison with field data. *Journal of Wind Eng. and Ind. Aerodynamics*, Vol. 64, pp. 221-231.
- Deterling, H. and D. Etling, 1984. Application of the E- ϵ Turbulence Model to the Atmospheric Boundary Layer. *Boundary Layer Meteorology*, Vol. 33, pp. 113-133.
- Duynkerke, P., 1987. Application of the E-, Turbulence Closure Model to the Neutral and Stable Atmospheric Boundary Layer. *Journal of the Atmospheric Sciences*, Vol. 45, no. 5, pp. 865-880.
- Easom, G., 2000. *Improved Turbulence Models for Computational Wind Engineering*. Doctoral Thesis: University of Nottingham, School of Engineering.

ERCOFTAC, 2000. *Best Practices Guidelines for Industrial Computational Fluid Dynamics*, Version 1.0. Ed. Casey, M. and Wintergerste, T.

Franke, J., C. Hirsch, A. Jensen, H. Krus, M. Schatzmann, P. Westbury, S. Miles, J. Wisse, and N. Wright, 2004a. Recommendations of the use of CFD in Predicting Pedestrian Wind Environment. *COST Action C14*, Working Group 2.

Franke, J., C. Hirsch, A. Jensen, H. Krus, M. Schatzmann, P. Westbury, S. Miles, J. Wisse, and N. Wright, 2004b. Recommendations of the use of CFD in Wind Engineering. *Proceedings of Urban Wind Engineering and Buildings Aerodynamics*, Brussels.

Garratt, J., 1992. *The Atmospheric Boundary Layer*. Cambridge University Press. New York.

Gao, Y. and W. Chow, 2005. Numerical Studies on Air Flow Around a Cube. *Journal of Wind Eng. and Ind. Aerodynamics*, vol. 93, pp. 115-135.

Grimmond, C. and T. Oke, 1999. Aerodynamic Properties of Urban Areas Derived from Analysis of Surface Form. *Journal of Applied Meteorology*, vol. 38, pp. 1262-1292.

Hall R., 1996. Evaluation of modelling uncertainty – CFD modelling of near-field atmospheric dispersion, *Project EMU final report*, WS Atkins Consultants Ltd, UK.

Hanna, R., O. Hansen, and S. Dharmavaram, 2004. FLACS CFD air quality model performance evaluation with Kit Fox, MUST, Prairie Grass, and EMU observations. *Atmospheric Environment*, vol. 38, pp. 4675-4687.

Hosker, R., Jr., 1984. Flow and diffusion near obstacles. *Atmospheric Science and Power Production*, Chapter 7. D. Randerson, ed. Department of Energy DOE/TIC-27601 (DE84005177), pp. 241-287.

Huber, A., W. Tang, A. Flowe, B. Bell, K. Kuehlert, and W. Schwarz, 2004: Development and Applications of CFD Simulations in Support of Air Quality Studies Involving Buildings. *Proceedings of 13th Conference on Applications of Air Pollution Meteorology*, AWMA/AMS.

Huser, A., P. Nilsen, and H. Skatun, 1997. Application of the K- ϵ Model to the Stable ABL: Pollution in Complex Terrain. *Journal of Wind Eng. and Ind. Aerodynamics*. vol. 67 & 68, pp. 425-436.

Kato, M. and B.E. Launder, 1993. The modeling of turbulent flow around stationary and vibrating square cylinders, *Proc. 9th Symposium on Turbulence and Shear Flows*, Kyoto.

Kantha, L. and C. Clayson, 2000. *Small Scale Processes in Geophysical Fluid Flows*. Academic Press, San Diego, CA.

Kim, S. and F. Boysan, 1999. Application of CFD to environmental flows. *Journal of Wind Eng. and Ind. Aerodynamics*, vol. 81, pp. 145-158.

Kim, H. and V. Patel, 2000. Test of Turbulence Models for Wind Flow over Terrain with Separation and Re-circulation. *Boundary-Layer Meteorology*, vol. 94, pp. 5-21.

Lakehal, D. and W. Rodi, 1997. Calculation of the flow past a surface-mounted cube with two-layer turbulence models. *Journal of Wind Eng. and Ind. Aerodynamics*. vol. 67-68, pp 65-78.

Launder, B. and D.B. Spalding, 1974. The numerical computation of turbulent flows, *Computational Methods of Applied Mechanical Engineering*, vol. 3, pp. 269-289.

McAlpine, J.D. and M. Ruby, 2004. Using CFD to Study Air Quality in Urban Microenvironments. Chapter 1 of *Environmental Science and Environmental Computing*, Vol. II (P. Zannetti, Ed.) The Envirocomp Inst.

Meroney, R., B. Leidl, S. Rafailidis, and M. Schatzmann, 1999. Wind-tunnel and numerical modeling of flow and dispersion about several building shapes. *Journal of Wind Engineering and Industrial Aerodynamics*, vol. 81, pp. 333-345.

Minson, A., C. Wood, and R. Belcher, 1995. Experimental Velocity Measurements for CFD Validation. *Journal of Wind Eng. and Ind. Aerodynamics*, vol. 58, pp. 205-215.

Murakami, S. and A. Mochida, 1989. Three-Dimensional Numerical Simulation of Turbulent Flow Around Buildings using the K- ϵ Turbulence Model. *Building and Environment*, Vol. 24, No.1, pp. 51-64.

Murakami, S., 1998. Overview of turbulence models applied in CWE-1997. *Journal of Wind Engineering and Industrial Aerodynamics*, vols. 74-76, pp. 1-24.

Murakami, S., 2002. Setting the scene: CFD and symposium overview. *Wind and Structures*, Vol 5, No. 2-4, pp. 83-88.

QNET-CFD website, 2005. <http://www.qnet-cfd.net/>. Accessed 12-10-2005.

Ratcliff, M. and J. Peterka, 1990. Comparison of Pedestrian Wind Acceptability Criteria. *Journal of Wind Eng. and Ind. Aerodynamics*, vol. 36, pp. 791-800.

Richards, P. and R Hoxey, 1993. Appropriate Boundary Conditions for Computational Wind Engineering Models Using the K- ϵ Turbulence Model. *Journal of Wind Eng. and Ind. Aerodynamics*, vol. 46 & 47, pp. 145-153.

Riddle, A., D. Carruthers, A. Sharpe, C. McHugh, and J. Stocker, 2004. Comparisons between FLUENT and ADMS for atmospheric dispersion modeling. *Atmospheric Environment*, vol. 38, 1029-1038.

Sagrado, A., J. van Beeck, P. Rambaud, and D. Olivari, 2002. Numerical and experimental modelling of pollutant dispersion in a street canyon. *Journal of Wind Eng. and Ind. Aerodynamics*, vol. 90, pp. 321-339.

Scanlon, Thomas J., 1997. A Numerical Analysis of Flow and Dispersion Around a Cube. *Proceedings of IBPSA Building Simulation '97 conference*, Prague, Sept. 8-10, 1997.

Scaperdas, A. and S. Gilham, 2004. Thematic Area 4: Best Practice Advice for Civil Construction and HVAC. *QNET-CFD Network Newsletter*, Vol. 2, No. 4, July 2004.

Shih, T., W. Liou, A. Shabbir, Z. Yang, J. and Zhu, 1994. A New K- ϵ Eddy Viscosity Model for High Reynolds Number Turbulent Flows. *Computers and Fluids*, Vol. 24, No. 3, pp. 227-238.

Snyder, W., 1979. *The EPA Meteorological Wind Tunnel: Its Design, Construction, and Operating Characteristics* (EPA-600/4-79).

Snyder, W., 1981. *Guideline for Fluid Modeling of Atmospheric Diffusion* (EPA-600/8-81-009).

Snyder, W. and R. Lawson, 1994. Wind-tunnel Measurements of Flow Fields in the Vicinity of Buildings. *Proceedings of the 8th AMS/AWMA Joint Conference on Applications of Air Pollution Meteorology*. Jan. 23-28, 1994. Nashville, Tennessee.

Stathopoulos, T., 2002. The numerical wind tunnel for industrial aerodynamics: Real or virtual in the new millennium? *Wind and Structures*, Vol. 5, No. 2-4, pp. 193-208.

Stull, R., 1988. *An Introduction to Boundary Layer Meteorology*. Kluwer Academic Publishers, Netherlands.

Tang, W., A. Huber, B. Bell, K. Kuehlert, and W. Schwarz, 2005. Example Application of CFD Simulations for Short-Range Atmospheric Dispersion over the Open Fields of Project Prairie Grass. *Proceedings of AWMA 98th Annual Conference*. Minneapolis, MN. June 21-25, 2005.

Tang, W., A. Huber, B. Bell, and W. Schwarz, 2006. Application of CFD Simulations for short-range atmospheric dispersion over open fields and within arrays of buildings. *Proceedings of AWMA/AMS 14th Joint Conference of the Applications of Air Pollution Meteorology*, Atlanta, GA, Jan. 30-Feb 2, 2006.

Tsuchiya, M., S. Murakami, A. Mochida, K. Kondo, and Y. Ishida, 1996. Development of New K-, Model for Flow and Pressure Fields Around Bluff Body. *2nd Int. Symposium on Computational Wind Engineering*, Col. State U. August 4-8, 1996.

Turner, D.B., 1970. *Workbook on Atmospheric Dispersion Estimates*. U.S. Environmental Protection Agency (AP-26).

Zhang, Y., S. Arya, A. Huber, and W. Snyder, 1992. *Simulating the Effects of Upstream Turbulence on Dispersion Around a Building* (EPA/600/A-92/228).

Zhang, Y., S. Arya, and W.H. Snyder, 1996. A Comparison of Numerical and Physical Modeling of Stable Atmospheric Flow and Dispersion Around a Cubical Building. *Atmospheric Environment*, Vol. 30, No. 8, pp. 1327-1345.